ANALYSIS OF EFFICIENT REGIONS FOR WIND POWER GENERATION IN KAZAKHSTAN

Anuar Aryngazin, B.Eng. Space Technique and Technology

Submitted in fulfillment of the requirements
for the degree of Master of Science
in Mechanical & Aerospace Engineering

School of Engineering and Digital Sciences
Department of Mechanical & Aerospace Engineering
Nazarbayev University

53 Kabanbay Batyr Avenue,
Astana, Kazakhstan, 010000

Supervisor: Assistant Professor Yerkin Abdildin
Co-supervisor: Assistant Professor Yerbol Sarbassov

May 2024

DECLARATION

I hereby, declare that this manuscript, entitled "***Analysis of Efficient Regions for Wind Power Generation in Kazakhstan***", is the result of my own work except for quotations and citations, which have been duly acknowledged.

I also declare that, to the best of my knowledge and belief, it has not been previously or concurrently submitted, in whole or in part, for any other degree or diploma at Nazarbayev University or any other national or international institution.

_____

Name: Anuar Aryngazin

Date: 02.05.2024

Abstract

Global concerns about climate change and the decreasing of fossil fuels reserves have made renewable energy production a major priority. Wind energy is a well-established research area. However, identifying optimal regions for wind power production requires weighing multiple factors, including wind speed, density, availability, and the environmental consequence of reducing greenhouse gas (GHG) productions, and application of decision analysis. The main purpose of this study is to analyze the regions of Kazakhstan and identify the optimal location for

wind energy production using the decision analysis extension of multiattribute utility theory (MAUT). Previous literature conducted analyzing wind power potential in Kazakhstan has identified several promising locations for efficient wind energy production. However, the selection process did not involve mathematical analysis; instead, the choice was primarily determined by quantitative results obtained from empirical studies. This study identified seven favorable areas based on expected utility and a comprehensive study was conducted using the multiattribute utility function (MUF). This method facilitated the selection of wind energy projects in efficient regions, taking into account factors such as potential power production and GHG emission reduction potential. The study involves collecting data on the GHG emission reduction potential and wind speed, followed by analysis and decision making to identify practical wind energy projects. Moreover, the data analysis includes a questionnaire for the decision maker (DM). This made it possible to determine the optimal locations for installing wind farms based on the real preferences of an expert in the field of energy. The results based on the expected utility values showed that the most optimal location for installing a wind power plant is Fort-Shevchenko and Yereymentau. The results of the research project are critical for the development of wind energy in Kazakhstan and for identifying the most efficient regions for wind energy production using utility theory. This study contributes to the development of wind energy in Kazakhstan and provides information for decision-making processes on sustainable energy production.

Acknowledgements

I extend my sincere gratitude to my Professor and Supervisor, Yerkin Abdildin, for his supervision and feedback during this research. I appreciate his support in shaping the direction of study, providing valuable feedback, contributing to the improvement of this work. I also express my thanks to my co-supervisor, Professor Yerbol Sarbassov, for his help and insightful feedback

throughout this study. Finally, I would like to thank all the participants that contributed to this study, without them this research would not have been possible.

Table of Contents

List of Abbreviations & Symbols

CDF Cumulative density function
DA Decision analysis
DM Decision maker
DT Decision tree
EPFM Energy pattern factor method
GHG Greenhouse gas
GWP Global warming potential
IEC International electrotechnical commission MAUT
Multiattribute utility theory
MUF Multiattribute utility function
MUI Mutual utility independence
NREL National Renewable Energy Laboratory PDF
Probability density function
PUI Partial utility independence
PV Photovoltaic
RES Renewable energy resources
RMSE Root mean square error
UDM Utility dependence matrix
UI Utility independence
WMO World meteorological organization
WPD Wind power density
WPP Wind power plant
WSC Wind shear coefficient

List of Tables

List of Figures

Chapter 1 – Introduction

1.1. Research objectives

The primary goal of this research work is to formulate a mathematical model aimed at identifying optimal locations for the installation of wind power plants (WPP) in Kazakhstan. The key objectives include the exploration and examination of the power output of wind energy and GHG emission decrease potential across the territory of Kazakhstan, which is relevant in the energy sector. To apply the mathematical decision-making methodology, the Multiattribute Utility Theory (MAUT) will be employed. This involves the calculation of statistical data of each location's potential power output and GHG emission reduction potential, specifically their minimum, low, base, high, and maximum values. The MAUT decision analysis methodology involves a decision maker (DM) who will be identified to participate in the study by responding to questionnaires. The results of the true preferences of DM, who is normally an expert in the corresponding field, will significantly influence the ultimate determination of the optimal location for WPP installation.

The identification of influential factors (i.e. attributes) forms an initial part of this research problem. Specifically, there will be two attributes, denoted as X_1 – potential wind power output and X_2 – GHG emission reduction potential. In addition, the MAUT methodology involves the construction of a decision tree (DT). This allows a graphical representation of the decision sequence that demonstrates the expected multiattrubute utility value of each alternative. Moreover, the development of questionnaires designed to evaluate the preferences of DM, along with additional research to find the dependencies among the attributes will be used in the research.

Finally, the MUF will be constructed and all alternatives will be ranked by the expected utility, ultimately identify the most suitable places for the setting up a WPP. Key research questions that will be explored during this study:

- Which regions and locations in Kazakhstan are preferable for installing wind power plants that were formulated by the multiattribute utility theory methodology (MAUT)?
- How can decision analysis and MAUT help in choosing the optimal locations for installing wind power plants?

1.2. Background

Generation of electricity is a critical part of the modern world, ensuring global electrical sustainability and stability. Nowadays, the global society dependent on energy. All social structures must ensure that the basic needs for energy are satisfied. These needs encompass vital aspects such as healthcare, water, illumination, sustenance, transportation, and the creation of a generally conducive energy environment [1]. Moreover, there are still a certain part of the region with people who do not have access to electricity consistently. The count of individuals without consistent access to energy increased from 754 million in 2021 to an estimated 774 million people

in 2022 [2]. According to data from the UN Population Division (2022), this is nearly 9.7% of the global population as of the latest available records [3]. According to IEA, the global electricity demand reached 728 terawatt-hours (TWh), showing a notable increase compared to 2022 at 590 TWh [4]. The report further forecasts that by 2025, global electricity demand is expected to reach

900 TWh [4]. This highlights the growing significance of consistent energy sources in meeting the world's rising power needs.

The global energy production can be categorized into three main groups: traditional fossil fuels, nuclear sources, and renewable energy sources (RES). According to IEA, more than 65% of electricity generation comes from traditional energy sources [5]. In contrast, RES accounted for nearly 25% of the global electricity generation, while nuclear power contributed to approximately 10% [5].

Nevertheless, traditional energy production using fossil fuels leads to significant production of GHG emissions. The production of anthropogenic GHG emissions represents a crucial challenge in contemporary energy systems. Al-Ghussain et al. (2019) exposed that the relentless consumption of hydrocarbon resources for energy generation has resulted in a significant upsurge in GHG concentrations worldwide [6]. Furthermore, this study emphasizes that increased carbon dioxide (CO_2) emissions directly correlate with the growth of key climate change indicators. Environmental pollution and climate change have, for decades, remained the preeminent global concerns. Over the past two decades, the climate has witnessed a profound transformation. For instance, in 2022, the global average surface temperature rose by a significant 1.15°C [7]. The implications of climate change, a consequence of mineral extraction for energy production, ripple far and wide, impacting all countries across the globe. The WMO has

established pivotal indicators that aptly reflect the world environment condition [8], [9]. These metrics include global mean surface temperature, ocean heat content, acidification status, global ocean absorption of CO_2, and global mean sea level [8], [9]. Notably, these metrics are intricately interconnected, so any incline in one can induce changes in others. For instance, if global CO_2 emissions continue to rise at the current pace, the global mean surface temperature could potentially exceed the 1.5°C - 2.0°C threshold by 2030 [8]. Moreover, human activity, especially the GHG emissions from sources like coal, oil, and gas, is a leading driver of climate change. In the report of IEA (2023) it is noted that CO_2 emissions stemming from energy-related activities exhibited a 0.9% increase, surging to surpass approximately 37 gigatons (Gt) in 2022, which makes a new maximum record of CO_2 emissions [10]. A study by Rossati (2017) has revealed that climate change adversely affects soil quality, degrades agriculture, and reduces the availability of fresh water, thereby harming economies and citizens, especially in low-income

nations [11]. The sustainability of economies, environmental security, and social well-being in countries is at significant risk. Moreover, the World Bank has estimated that all geophysical activities may cost the world over US$500 billion annually [12].

Anthropogenic carbon dioxide emissions into the Earth's atmosphere result from a number of primary sources. The data that was used to quantify the sources of GHG emissions worldwide are displayed in Figure 1 [13]. This shows that the production of energy accounts for a sizable 73% of CO_2 emissions.

The severe impacts of human-caused climate change are negatively impacting the global energy sector and require coordinated action. The UN General Assembly 2015 presented the crucial SDGs that provide a sustainable and reliable energy environment and reduce the carbon footprint (SDG 7 – Affordable and Clean Energy, SDG 13 – Climate Action)) [14]. RES – one of critical solutions to the worldwide challenges of decarbonization and progression of sustainable development. Many research findings declare a strong reliance on RES aligned with current sustainability and environmental principles within the worldwide energy industry [15], [16], [17], [18]. They assert that renewable energy sources are environmentally friendly, as they do not generate negative effects on the atmosphere and positively affect the reduction of global GHG

emissions [15], [16], [17], [18].

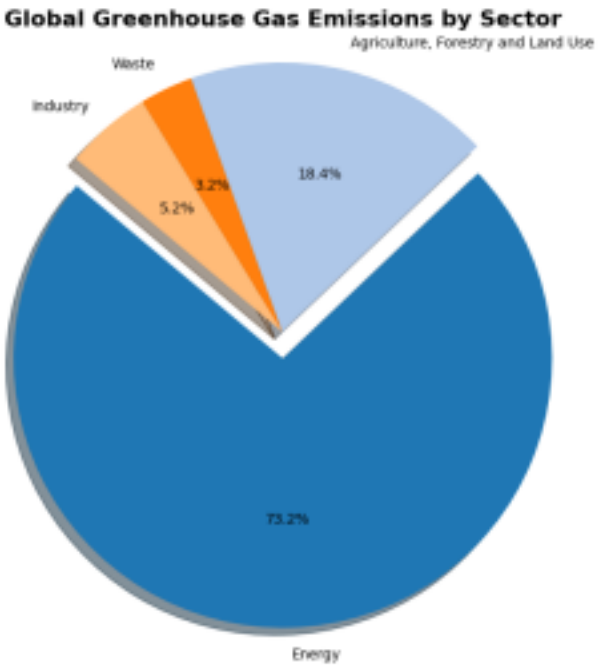

Figure 1. Global greenhouse gas emissions by sector. Source: Adapted from [13].

Figure 2 illustrates a graph of the growth trend of the total RES energy capacity from 2013 – to 2022 and energy production 2013 – 2021 [19]. It is obvious that over the years, RES have led the development energy sector which emphasizes their significant role in combating climate change.

Considering the energy industry, one of the main objectives is to reduce CO_2 emissions, known as decarbonization, through achieving green and sustainable advancement [16], [18]. Empirical evidence indicates a trend of declining energy consumption as prices for fossil fuel based energy resources rise [16]. To facilitate a comprehensive and equitable shift towards this goal, authors suggest implementing a worldwide tax on energy derived from processes that release CO_2 gases, as an instrument to reduce the carbon footprint [16], [18]. It is possible that by raising the price of carbon emissions, an economic incentive could be created for governments and the energy industry to switch to cleaner, renewable energy sources. The authors also indicate that the reduction of CO_2 emissions and the widespread implementation of RES and sufficient energy infrastructure will mitigate negative impacts on the climate, ultimately facilitating the achievement of the goal to limit global warming to one and a half degrees Celsius [16], [18].

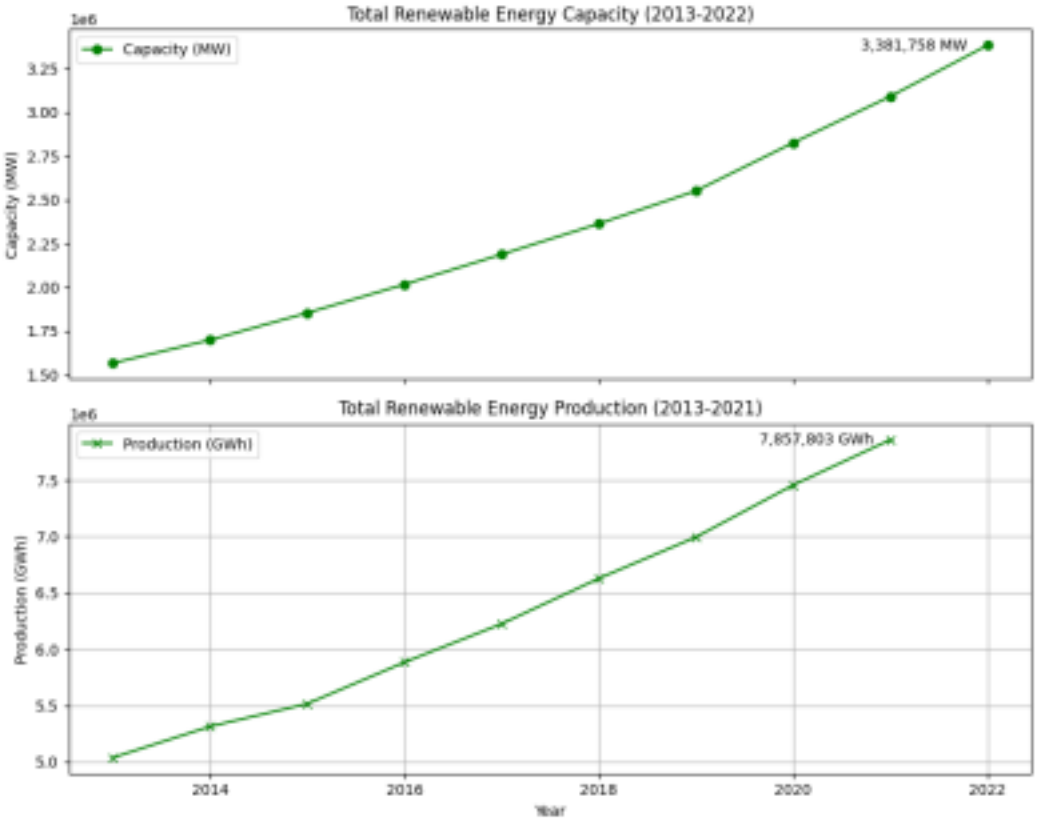

Figure 2.
Total Renewable Energy Capacity and Renewable Energy Production in the World from 2013 to 2022 (to 2021 for Production), in Megawatts (MW) and Gigawatt hour (GWh). Source: Data from [19].

The 1.5 C target, as developed by the Paris Agreement in 2015, is an essential climatic goal to prevent the worst consequences of climate change [20]. Moreover, IRENA estimates that one gigawatt-hour (GWh) of renewable energy could potentially reduce carbon dioxide emissions by an average of more than three million tons [21]. In a report dated 2022, the IEA calculated that about 550 million tons of carbon dioxide emissions were kept out of the earth's atmosphere, mostly due to technological advancements in solar photovoltaic and wind generating (overall reduction estimate – approximately 465 million tons of CO_2) [22]. They claim that without the RES technology growth trend, annual CO_2 emissions might triple. Transitioning to RES is a fundamental step and the widespread adoption of alternative sources, coupled with carbon emission tax pricing, can possibly create a strong synergy in combating against reducing the carbon footprint.

1.3. Types of renewable energy sources

The development of the fundamental types of RES can be related to the progress made in technology over the past 50 years and the growing concern over environmental degradation. Among the major RES that are currently known are solar energy, geothermal energy, hydropower, wind power, and bioenergy [21], [23]. The following paragraphs will explore types of RES.

Wind energy.

Wind energy was used in ancient times at least three thousand years ago [24], for transporting boats [24] and crushed grain [23], in modern times wind energy with turbines is used to generate power. For example, in 2021, wind power provided almost 50% of the world's clean electricity production, which is approximately 18.5 million GWh and growing. Wind energy is a sustainable source of electricity, with numerous advantages over traditional fossil fuel-based electricity power generation. Wind energy significantly reduces GHG, as 1 MW wind turbine can offset 2,400 tons of CO_2 [25]. Additionally, wind power does not produce particulates, which are detrimental to human well-being and the environment, unlike coal-fired power stations. Wind turbines are versatile in location, allowing them to be erected in areas such as mountaintops, pastures, or along major roads without disrupting other land uses [25]. This flexibility minimizes conflicts with urban development and preserves valuable land for various purposes. To sum up, wind energy presents a compelling solution to environmental and energy challenges. Its ability to reduce emissions, its versatile location options, and its potential to reduce the impacts of fossil fuel make it a sustainable and cost-effective choice for the future of electricity generation.

Solar energy.

Solar energy is one of the main alternative and clean energy sources derived from clean and almost infinite resource. Solar energy, as many sources believe, is one of the most promising RES, due to its efficiency properties, as well as great functionality [15], [17], [18], [21], [23]. For instance, solar energy using photovoltaic (PV) systems can reduce CO_2 emissions by up to 100 million tons [21]. Furthermore, solar energy can serve a dual purpose by not only facilitating energy storage but also functioning as a liquid heating system and a desalination method [23]. PV panels are used to convert solar irradiation directly into electricity [23]. Furthermore, cooling

systems provide cooling capabilities, while thermal energy for buildings is collected, saved, and distributed through heating technologies [26]. Moreover, the thermal energy derived from RES such as solar energy is harnessed for the purpose of evaporating water and removing salt, which in turn produces fresh water [23]. As solar energy progresses in terms of its economic impact, the production cost continues to decrease consistently [27], [28]. To summarize, solar energy is a major alternative and green source of energy, with almost infinite resource potential, as well as a wide range of applications.

Hydro energy.

Hydropower is an environmentally clean and cost-effective renewable energy source (RES). Hydroelectric power generation involves capturing the energy of water flowing from a higher elevation, which possesses significant potential energy, to drive a hydraulic turbine, thereby producing mechanical work that is subsequently transformed into electricity using a connected generator [23]. A key benefit of hydro energy is its capacity for immediate utilization and simultaneous exploitation [23]. Overall, hydropower remains a valuable component of the renewable energy landscape, but its sustainability depends on responsible development and management practices.

Bioenergy.

Bioenergy is one of the types of RES that uses organic materials to generate electricity. Bioenergy, derived from biomass consisting of organic matter, represents a versatile and sustainable renewable energy source [21],[29]. A wide variety of organic resources can be utilized in the biofuel manufacturing process, including microalgae, agricultural wastes, food waste, leftover wood, forest debris, and different kinds of grasses and others [23], [29]. Bioenergy has a wide range of applications: for instance, in the transportation sector, including vehicles and biofuel production, as well as in residential and industrial settings [23]. Its uses encompass heating and the generation of general thermal energy. Overall, bioenergy represents an environmentally friendly and multifaceted RES.

Geothermal energy.

Geothermal energy is another type of RES, representing a reliable source of energy. To extract geothermal energy, the thermal energy of the hot layers of the Earth is applied in combination with turbines and generators [23]. Geothermal power plants can operate all the time, delivering a steady stream of electricity, which can be especially vital for regions that require a continuous energy source. Moreover, geothermal energy is a sustainable option with a low environmental impact. It produces minimal GHGs and has a small footprint compared to many other forms of energy generation [23], [29]. In conclusion, geothermal energy stands as a sustainable and ecologically friendly type of RES.

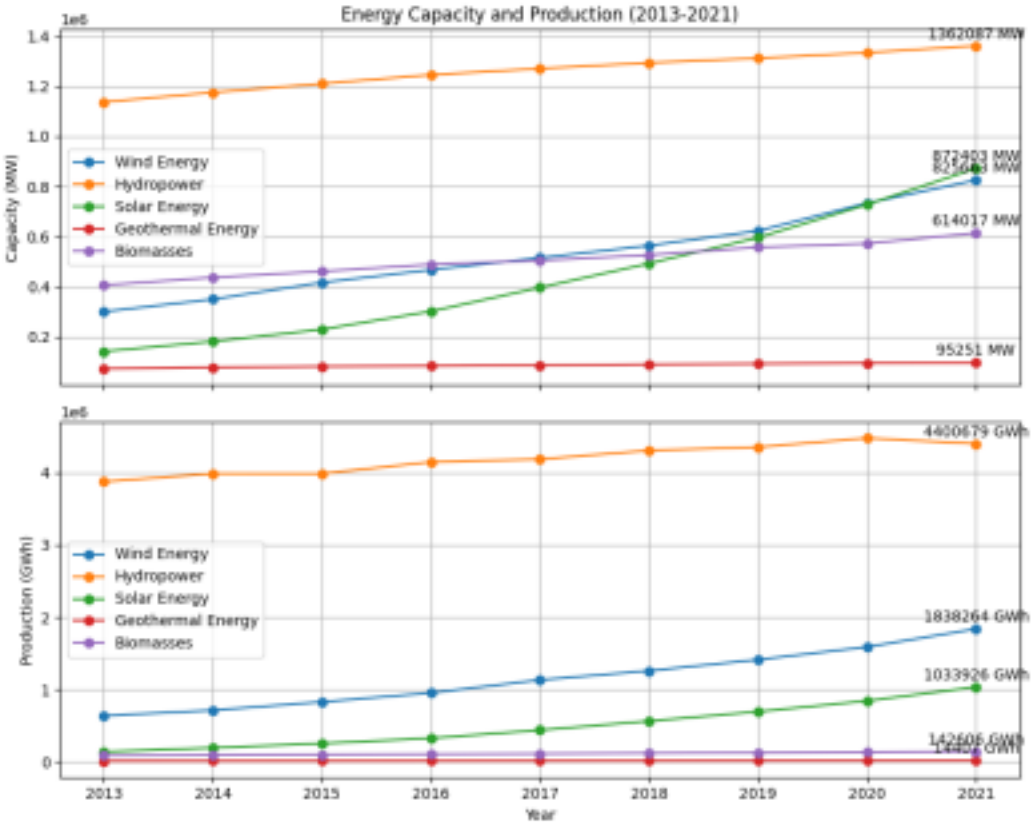

Figure 3. Total Renewable Energy Capacity and Production for five types of RES in the

World, ranging from 2013 to 2021, in Megawatts (MW) and Gigawatt hours (GWh). Source: Data from [19].

Figure 3 shows the total production and capacity of five types of RES from 2013 to 2021. Firstly, hydropower clearly dominates in both production and capacity, consistently outperforming

other renewable energy options throughout the period under review, with over 4400 TWh produced in 2021. This shows the established use of hydropower as a reliable source of renewable energy. Secondly, wind and solar energy are becoming the next most important contributors to RES. Wind energy production has outpaced solar energy in production, with production at 1,838,264 GWh compared to 1,033,926 GWh in 2021. This suggests that the wind industry has made significant progress in harnessing wind energy to produce electricity and remains a major contributor to the renewable energy sector. However, it is important to recognize that both bioenergy and geothermal energy are lagging significantly in terms of production, with both continuously falling below 150,000 GWh in 2021.

This study will focus on exploring the implementation of wind energy and the integration of decision analysis for choosing the best location for wind turbines installation to accelerate the sustainable energy development in Kazakhstan. Despite various studies highlighting the significant potential of solar energy and other forms of RES as the main energy sources in Kazakhstan, this study focuses on wind energy in this particular environment, as wind energy is well suited for this region [30], [31], [32], [33], [34], mainly due to the wide variety of suitable locations for installing wind turbines and significant wind resources available in many regions of the country. Consequently, this study will primarily investigate the wind energy.

Chapter 2 – Literature Review

The literature review section of this study aims to provide an overview of the existing research on the study of potentially efficient regions for wind power generation in Kazakhstan, and the application of multiattribute utility theory (MAUT) as a decision-making tool. This section will discuss the potential of wind power generation potential in the regions of Kazakhstan. After this section will review the methodologies of previous studies, and discuss the results, comparing and contrasting results to identify the most efficient regions for wind energy production. The advantages and limitations of using a multiattribute utility function (MUF) for decision analysis will also be discussed. In addition, the factors affecting the efficiency of wind energy production in Kazakhstan will be considered. Overall, this section aims to identify knowledge gaps and structure the future research in this area.

2.1. Renewable energy sources in Kazakhstan

Kazakhstan is located in Central Asia, boasts an extensive landmass covering more than 2.7 million square kilometers, ranking it as the 9th largest country on the global scale [35].

Kazakhstan is a sizable nation with many and diverse natural resources, all of which have tremendous energy potential. Many sources claim that Kazakhstan is favorable country for the installation of RES, especially wind farms [6], [8], [9], [11], [12], [36], [37]. The country has a range of favorable wind patterns that make it a suitable location for wind farms. According to the Ministry of Energy of the Republic of Kazakhstan, in 2021 there were 116 renewable energy sources (RES) operating in Kazakhstan with an installed capacity of approximately 1,700 MW. At the end of 2020, more than 3 billion kWh of energy were produced [38]. By increasing renewable energy sources (RES) in Kazakhstan, this region has the potential to decrease its dependence on traditional energy sources, and contributing reduction of CO_2 emissions and assisting in the climate change impacts.

2.2. Wind Energy in Kazakhstan

Kazakhstan has the potential to become a significant player in the wind power industry. Figure 4 illustrates the average wind speed in Kazakhstan for 2022 at a height at 100 meters, most of the country's territory yearly averages 7 — 7.5 meters per second, and Figure 5 at height of 50 meters

with an average wind speeds of 6 — 6.5 m/s respectfully [39]. Since the power output of a wind turbine is directly proportional to the cube of the wind speed, this means that, the higher the wind speed, the more energy a WPP can generate [40]. Therefore, this region has great wind power potential, which emphasizes the value of investigating and expanding the RES in Kazakhstan.

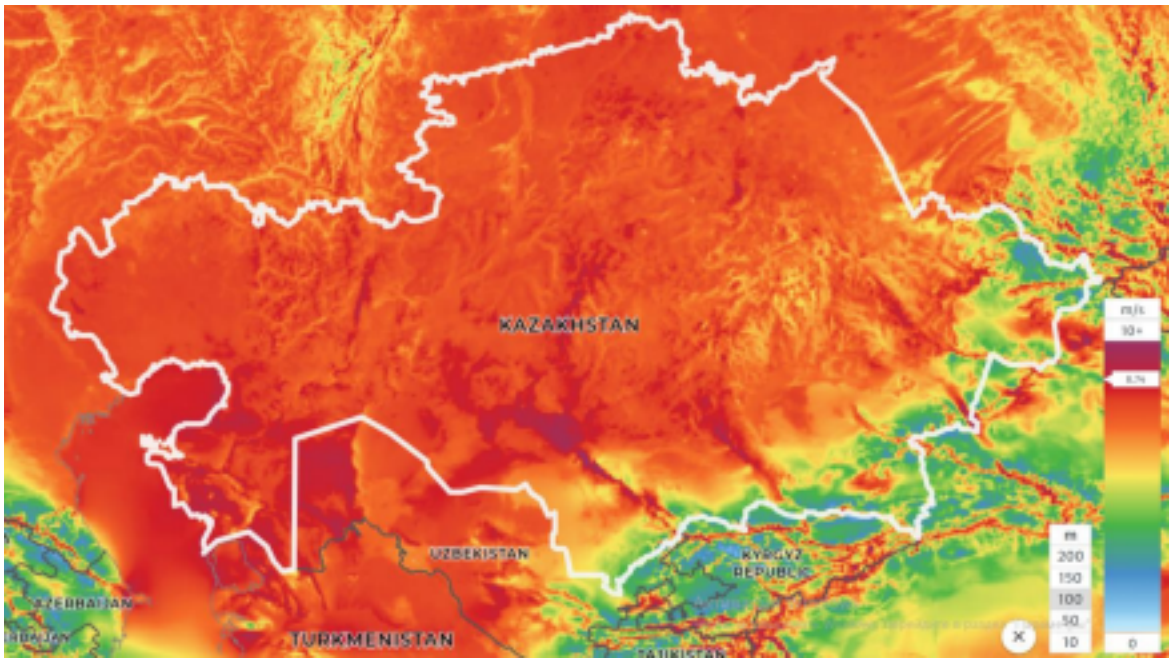

Figure 4. Map of wind speed in Kazakhstan at 100 meters' height (Red is more than 10 m/s Yellow is 5 m/s Blue less than 1 m/s). Source: [39].

Kazakhstan is an upper income country with rapid economic growth [41]. This rapid expansion, however, comes with an associated surge in demand and energy consumption within the nation. The elevated economic activity and development in various sectors contribute to an increased need for energy resources. The extensive landscapes of Kazakhstan offer a substantial potential for the installation of wind energy systems, considering the vast wind resources available [31]. The great wind patterns of Kazakhstan make it possible to implement alternative renewable energy, specifically wind power [34], [37], [42]. Currently the number for operating renewable energy plants is 134 with a total capacity of 2010 MW, while the amount of generated electricity from the renewable energy facilities reached about 4,2 billion kWh in 2021 [31]. Karatayev and Clarke, 2016 claimed that the northern and central regions around the Caspian Sea have the biggest wind potential [34].

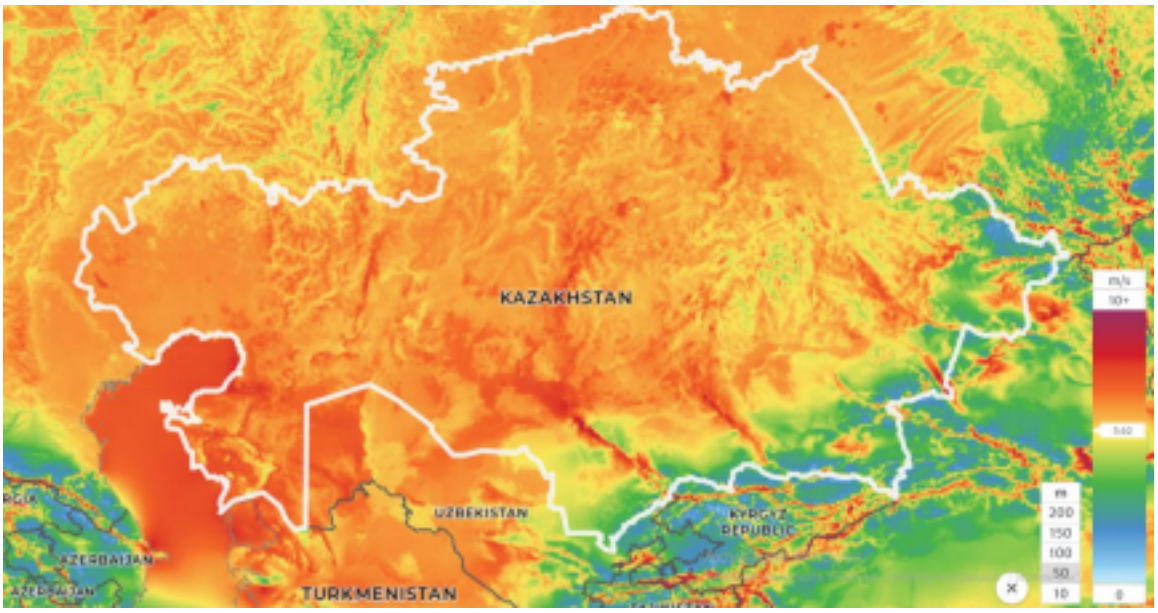

Figure 5. Map of wind speed in Kazakhstan at 50 meters' height (Red is more than 10 m/s Yellow is 5 m/s Blue less than 1 m/s). Source: [39].

The regulatory framework established by the Kazakh government reflects a commitment to renewable energy, fostering an environment suitable for the growth of wind energy projects [43]. In 2023 in the meeting of "Kazakhstan-European Union" the Prime Minister stated that Kazakhstan is highly interested in leading a sustainable economy by increasing the proportion of renewable energy sources to 15% by the year 2030 [44]. Additionally, the implementation of favorable tariffs for wind energy production acts as a catalyst, stimulating private investments in this sector [45]. According to the law "On Support for the Use of Renewable Energy Sources" the producers of RES are able to distribute at special tariffs through the RES Settlement and Financial Support Center to the public network [46]. The feed-in tariffs for the purchase of wind power stations is estimated by 22,7 tenge/kWh (without VAT) or 0.05 US dollars (1 USD = 450 tenge) [47]. The convergence of geographical advantages, supportive regulations, and attractive tariffs positions Kazakhstan an attractive country for private investors entering the wind energy sector. The government's commitment to diversifying its energy source mix aligns with the global shift towards sustainable practices, presenting an opportunity for private entities to contribute and benefit from Kazakhstan's renewable energy initiatives.

2.3. Previous studies that identified efficient regions

Many studies have suggested efficient regions for wind power generation in Kazakhstan [30], [31], [32], [34], [42], [48], [49]. Various studies have been conducted to identify the most suitable locations for wind power generation in Kazakhstan. For instance, a study by Laldjebaev et al. [30] asserts that among all of the countries in Central Asia, Kazakhstan has the greatest potential for producing wind energy. To organize the information from the reviewed literature, a synthesis matrix was produced in the Table 1, which included relevant details from each study, citation, the regions identified as having high wind power potential, and the factors influencing wind power efficiency in Kazakhstan from 2007 to 2021.

All studies from 2007 to 2021 from the methodology had the primary attributes for determining the optimal locations: the average wind speed, energy production, economic potential and height below 100 meters. However, studies by Jianzhong et al., 2018 [31] and Turgali et al., 2021 [50] have an additional attribute used - GHG emission reduction. This attribute is not correlated with wind speed, height, energy production potential, and other attributes that were used in other researches.

As can be seen from the Table 1, many studies indicate that potentially optimal places for installing wind turbines are the gates of Dzungarian Gate, Shelek (formerly Chilik), Yereymentau, and along the Caspian Sea, and the city of Astana [30], [31], [32], [34], [42], [48]. In addition, in the study [49], suitable locations such as Fort-Shevchenko, Atbasar, and Akmola are proposed in the north side and west sides of Kazakhstan. These studies have identified regions with high wind power potential, which can be further explored for wind power projects. Decision makers can use the results of these studies in the energy sector to identify suitable locations for wind power projects in the country. However, further research using other decision analysis methods such as MAUT, is needed to comprehensively analyze the most efficient areas for wind power generation in Kazakhstan.

Table 1: Studies that identified the optimal locations of wind power generation in Kazakhstan 2007-2021 Sources: *[30], [31], [32], [34], [42], [48], [49]***.**

Citation	*Identified Optimal Locations Attributes*
	1. Dzungarian Gate 2. Shelek (formerly Chilik) 3. Along Caspian Sea 4. Astana
	1. Yereymentau 2. Fort-Shevchenko 3. Chilik 4. Astana 5. Karabatan
	1. Dzungarian Gate 2. Chilik
	1. Dzungarian Gate 2. Saryzhas–Zhuzimdyk–Taraz corridor 3. Caspian corridor 4. Emba corridor 6. Astana– Yereymentau corridor 5. Urzhar corridor
	1. Mangystau mountains 2. Peak Karatau 3. Chu-Ili mountains 4. Mount Ulytau 5. Yereymentau mountains 6. Mugojary mountains 7. Djungar gates
	1. Fort-Shevchenko 2. Atbasar 3. Akmola

Cochran, 2007 [48]	• Wind speed • Height		
		[30]	• Wind speed
Akhemtov et al., 2011 [42]		1. Dzungarian Gate 2. Mangystau Region 3. Karatau Region 4. Chu-Ili Mountains	Wind speed • Height • Wind speed • Wind availability • Height Economic Potential • GHG Emission Reduction Potential
Karatayev and Clarke, 2016 [34]			
Jianzhong et al., 2018 [31]			• Wind speed • Potential annual production of energy
Satuyeva et al., 2019 [32]			• Wind speed • Annual wind speed average • Potential production of energy
Pourasl and Khojastehnezhad, 2021 [49]			• Average wind speed • Potential production of energy
Laldjebaev et al., 2021	distribution • Wind speed changes at height • Potential power output •		

2.4. Multiattribute Utility Theory

The search for optimal locations for wind power plants involves a difficult decision-making process, involving factors such as wind potential, environmental impact, and economic feasibility. Among the various decision analysis methods, the Multiattribute Utility Function (MUF) stands out as a valuable tool for integrating diverse criteria into a comprehensive decision-making framework. The assessment of decisions can be facilitated through the application of Multiattribute Utility Theory (MAUT). Decision-making process involves the acquisition of information, the evaluation of possibilities, and ultimately, the selection of a course of action. According to Abbas [51], the decision-making process necessitates information gathering, comprehensive option assessment, and final decision making. To employ a Multiattribute Utility Function (MUF) for decision assessment, it is imperative to construct a well-defined decision scenario in which each alternative leads to a distinct outcome. Furthermore, the decision-making process, particularly when dealing with uncertain consequences, can benefit from Howard's proposed rules, such as the ordering and probability rules [52]. The MUF offers a structured framework for addressing intricate decision problems, enabling decision makers to account for multiple attributes and compare various alternatives. Utilizing the Multiattribute Utility Theory and decision trees, decision makers can evaluate the probabilities associated with different outcomes and determine the most favorable choice. In the context of this study, the application of MUF decision analysis empowers decision makers to assess diverse attributes and compare numerous alternatives, ultimately identifying the most efficient regions within the country for wind power generation. Nevertheless, no prior studies were identified that had applied the Multiattribute Utility Function (MUF) decision analysis method to select optimal places for wind farms. However, considering the potential of MUF decision analysis methods to provide a quantitative framework for addressing complex decision problems, further research is warranted to ascertain the suitable regions for wind power projects in Kazakhstan.

Chapter 3 – Methodology

In this section, the research methodology will be discussed, commencing with the software used, data collection and analysis of wind power metrics and GHG reduction potential. The subsequent steps include the systematic process of gathering relevant data, assessing the key metrics associated with wind power generation and potential power output, and estimating the potential reduction in greenhouse gas emissions. Following this, the analytical techniques applied to derive insights from the collected data will be detailed to ensure its accuracy and reliability. Lastly, the gathered and normalized data will be explained in terms of its utilization for the construction of the Multiattribute Utility Function (MUF). In the framework of this research, "Python" programming language and "Microsoft Excel" spreadsheet was used to carry out wind speed data analysis; geographic information system software "QGIS" was used to map the territory of Kazakhstan, highways, railways, network, cities and population, and to initially select areas for further investigation. In the following, all physical quantities will be measured in SI units unless otherwise specified.

3.1. Wind analysis: Weibull distribution

For wind data analysis Weibull distribution will be utilized. Many sources suggest to use Weibull distribution for the wind analysis because of its flexibility and reliability in aggregation of wind data [31], [49], [50], [53], [54], [55], [56], [57], [58], [59]. The two-parameter Weibull distribution is particularly well-suited for modeling wind speed data, because it allows the variability in wind speeds over time and can accurately describe the distribution of wind speeds at a specific location [31], [50]. The two parameters in this distribution are the scale parameter (c) and the shape parameter (k).

The following equation represents two-parameter Weibull distribution:

$$f(v) = \frac{k}{c}\left(\frac{v}{c}\right)^{k-1}\exp\left[-\left(\frac{v}{c}\right)^{k-1}\right], (k > 0, v > 0, c > 0) \quad (1)$$

where,

$f(v)$ – is probability of wind speed during the year;

v – wind speed, m/s;

k – shape parameter of distribution;

c – scale parameter of distribution.

Cumulative distribution function is determined by the expression:

$$F(v) = 1 - \exp\left[-\left(\frac{v}{c}\right)^{k}\right] \quad (2)$$

where $F(v)$ – is cumulative distribution function.

In the estimation of the Weibull parameters the Energy Pattern Factor Method (EPFM) will be utilized because of its accuracy and reliability in characterizing the wind energy distribution, compared to other estimation methods [53], [54], [59], [60], [61], [62].

The EPF is defined by the following expressions:

$$E_{pf} = \frac{\frac{1}{N}\sum_{i=1}^{N} v_i^3}{\left(\frac{1}{N}\sum_{i=1}^{N} v_i\right)^3} \quad (3)$$

$$k = 1 + \frac{3.69}{E_{pf}^2} \quad (4)$$

$$c = \frac{\bar{v}}{\Gamma\left(1 + \frac{1}{k}\right)} \quad (5)$$

where v – is wind speed, $\bar{v}$ – mean wind speed, Γ – is a gamma function.

The gamma $\Gamma(x)$ function in Equation (5) is determined by:

$$\Gamma(k) = \int_0^{\infty} k^{k-1} \exp(-k)\,dk \quad (6)$$

$$\Gamma(k) = \left(\sqrt{2\pi}\right)\left(k^{k-1}\right)\left(e^{-k}\right)\left(1 + \frac{1}{12k} + \frac{1}{288k^2} - \frac{1}{51840k^3} + \cdots\right) \quad (7)$$

The formula of Wind Power Density (WPD) based on the Weibull probability density function (PDF) is calculated by the following equation [61], [63]:

$$WPD = \frac{1}{2}\rho A^{3}\Gamma\left(1+\frac{3}{k}\right) \quad (8)$$

where ρ – is air density, A – is a scale factor, and k – is a shape factor.

The power output of wind turbine calculated by the expression [40]:

$$P_{output} = \frac{1}{2}\rho A^{2} v^{3} C_{p} \quad (9)$$

where ρ – is air density, A^{2} – is a swept area (A) of the wind turbine, r – blade length, v – is the speed of the wind, and C_{p} – is a capacity factor.

The capacity factor is calculated by:

$$C_{p} = \frac{P}{P_{max}} \quad (10)$$

where P_{output} – is a power output of a wind turbine, P_{max} – is a maximum power output at period of time by the wind turbine.

The coefficient that describes the losses of a wind turbine is determined by the following equation [50], [64]:

$$K = (1 - K_{a})(1 - K_{a\&i})(1 - K_{d})(1 - K_{o}) \quad (11)$$

where K_{a} – is an array losses, which are caused by the effect of the multiple wind turbines that stand next to each other, $K_{a\&i}$ – is the airfoil soiling and icing losses, which are caused by the weather condition effect on the wind turbine, such as ice on the blades, K_{d} – is the downtime losses, this type of losses in operational time occur due to planned maintenance, failures in wind turbines, plant downtimes, and utility outages, K_{o} –

miscellaneous losses, that caused by switching between the cut-out and cut-in wind speed values of wind turbines.

3.2. Wind analysis: Wind shear

To define the fluctuation of wind speeds at different heights, the Wind Shear variation or Wind Gradient equation will be employed. This meteorological phenomenon involves the gradual change in wind speed with increasing height and is needed for comprehending the vertical

distribution of wind energy [65]. It follows the rules of fluid mechanics when it comes to wind flows over the surface of the Earth, making it possible to analyze wind speed patterns using analytical and numerical methods [66]. The wind shear can be estimated by Hellmann power law equation [67]:

$$\text{□□}_2 = \text{□□}_1 (^{h_2}_{h_1})^{\text{□□}} \quad (12)$$

where □□_2 is a desired value of wind speed and height h_2 and □□_1 is a known value of wind speed at hub height h_1, and □□ is a wind shear coefficient (WSC) and can be calculated numerically, but usually this coefficient follows the power law of "1/7" meaning the value of □□ is usually 0.14 [65].

3.3. Wind analysis: Performance test

To ensure the quality of the data, the study will conduct two statistical error tests to ensure the reliability and accuracy of the data results. Testing for RMSE and R^2 will be carried out to the EPFM method that estimates two parameters k and c factors of the Weibull probability. Coefficient of determination (R^2) and root mean square error (RMSE), they characterize the quality and accuracy of the Weibull distribution [61]. The following equation determines the RMSE:

$$\text{□□□□□□□□} = \sqrt{\frac{1}{\text{□□}} \sum_{\text{□□}=1}^{\text{□□}} (\text{□□}_{\text{□□}} - \text{□□}_{\text{□□}})^2} \quad (13)$$

and to calculate R^2 the equation is used:

$$R^2 = 1 - \frac{\sum_{i=1}^{n} (y_i - f_i)^2}{\sum_{i=1}^{n} (y_i - \bar{y})^2} \quad (14)$$

where y_i – observed data frequency, f_i – experimental data frequency, $\bar{y}$ – mean value of observed data.

3.4. Wind analysis: Air density distribution

In the field of wind analysis, air density is main parameter in wind power generation calculations. To quantify air density, the Ideal gas law [68] for gas density will be used:

$$\rho = \frac{p}{R_s T} \quad (15)$$

where ρ – air density (kg/m^3), p – air pressure (Pa), R_s – specific gas constant for a dry air, $R = 287.05$ J/(kg*K) [69], and T – temperature (^{o}K).

In order to calculate the temperature T at specific height, such as wind turbines' hub height, the specific location's reference ground temperature is needed to be known. The lapse rate approximation formula calculates the temperature at specific height below 18 km above Earth's surface [70]:

$$T = T_0 - (h * \Gamma) \quad (16)$$

where T – temperature at desired height, T_0 – reference temperature, h – is a hub height, and $\Gamma = 0.0065$ K/m is the temperature lapse rate in the Earth's atmosphere.

To calculate the air pressure, barometric formula derived from Maxwell-Boltzmann distribution [71] is used:

$$p = p_0 e^{-\frac{g M (h - h_0)}{R T}} \quad (17)$$

where $$ – air pressure at height h, $$_0 –reference pressure at reference height h_0, $$ – universal gas constant $$ = 8.31432 N*m/(mol*K), $$ – acceleration of gravitational force ($$ = 9.8 m/s^2), and $$ – molar mass of the air $$ = 0.0289644 kg/mol.

To describe the normalized data to the specified hub heights, the Gaussian normal distribution probability and cumulative density functions will be utilized. The following equation describes the normal distribution's probability density function (PDF) [72]:

$$)^2 \quad (18)$$

$$(\quad) = \frac{1}{\sqrt{2}} ^{-\frac{1}{2}(\quad-\quad}$$

and the cumulative density function (CDF),

$$(\quad) = \frac{1}{\sqrt{2}} \int ^{-^2/2} \quad (19)$$

where $$ – is mean value, and $$ – is a standard deviation.

3.5. GHG reduction potential analysis

This subsection focuses on explaining the methodology for calculating GHG emission reduction potential as another attribute for the decision-making process. Assessing greenhouse gas emissions is an important step towards sustainable energy. Methodology applied using RETScreen Expert software is widely recognized and used in energy efficiency projects [64]. The following equation estimates the average annual greenhouse gas emissions reduction [64]:

$$\Delta = (\quad - \quad) \quad (1 - \lambda)(1 - \quad) \quad (20)$$

where $$ – is the base case of GHG emission factor , $$ – is the

proposed case of GHG emission factor, $\diamond\diamond_{\diamond\diamond\diamond\diamond\diamond\diamond\diamond\diamond}$ – is proposed case annual electricity produced, $\lambda_{\diamond\diamond\diamond\diamond\diamond\diamond\diamond\diamond}$– is the loss of electricity due to the transition and distribution, and $\diamond\diamond_{\diamond\diamond\diamond\diamond}$– is GHG reduction fee [64]. $\diamond\diamond_{\diamond\diamond\diamond\diamond\diamond\diamond\diamond\diamond}$ is calculated using following formula:

$$\diamond\diamond_{\diamond\diamond\diamond\diamond\diamond\diamond\diamond\diamond} = (\diamond\diamond_{\diamond\diamond\diamond\diamond 2}\,\diamond\diamond\diamond\diamond\diamond\diamond_{\diamond\diamond\diamond\diamond 2} + \diamond\diamond_{\diamond\diamond\diamond\diamond 4}\,\diamond\diamond\diamond\diamond\diamond\diamond_{\diamond\diamond\diamond\diamond 4} + \diamond\diamond_{\diamond\diamond 20}\,\diamond\diamond\diamond\diamond\diamond\diamond_{\diamond\diamond 20})^{\frac{1}{\eta}\frac{1}{1-\lambda}} \quad (21)$$

where $\diamond\diamond_{\diamond\diamond\diamond\diamond 2}$, $\diamond\diamond_{\diamond\diamond\diamond\diamond 4}$, and $\diamond\diamond_{\diamond\diamond 2\diamond\diamond}$ are the factors of GHG emission for the traditional type of electricity source, $\diamond\diamond\diamond\diamond\diamond\diamond_{\diamond\diamond\diamond\diamond 2}$, $\diamond\diamond\diamond\diamond\diamond\diamond_{\diamond\diamond\diamond\diamond 4}$, and $\diamond\diamond\diamond\diamond\diamond\diamond_{\diamond\diamond 20}$ are the global warming potentials for GHG emission components, η – is the fuel change efficacy, and λ – is the portion of power lost due to the transition and distribution [64]. The default $\diamond\diamond\diamond\diamond\diamond\diamond$ values for hundred year horizon defined by IPCC, 2007 [73] $\diamond\diamond\diamond\diamond\diamond\diamond_{\diamond\diamond\diamond\diamond 2} = 1$, $\diamond\diamond\diamond\diamond\diamond\diamond_{\diamond\diamond\diamond\diamond 4} = 25$, and $\diamond\diamond\diamond\diamond\diamond\diamond_{\diamond\diamond 20} = 298$.

In “RETScreen Expert”, estimated GHG emission factor excluding the transition and distribution (T&D) in Kazakhstan, which is 0,6363 tCO_2eq/MWh, and with the country-specific estimated T&D losses is equal to 7%, and the final GHG emission factor is equal to 0,6842 tCO_2eq/MWh. In order to describe the variability of the data the Gaussian distribution will be utilized (Equations 18-19).

3.6. Choosing locations for wind power generation

The process of selecting potentially effective wind energy generation sites plays an important role in the study. It involves careful evaluation based on specific criteria to ensure the practicality and effectiveness of the study. To determine the most suitable locations, a methodological approach was carried out that takes into account three key factors: wind resources, proximity to transport infrastructure and accessibility to densely populated areas [74].

The focus is on assessing wind resources at potential sites. The study uses the International

Electrotechnical Commission (IEC) wind classification, which focuses on locations with IEC wind turbine class III (7.5 m/s or higher) [75]. This assessment is carried out at both 50 and 100 meters to account for changes in wind speed and consistency at different heights. Further, proximity to transport infrastructure, especially highways. Efficient transportation is essential for the construction, maintenance and operation of a wind energy project. Consequently, sites are considered that are located within 5–10 kilometers from the nearest highway and at least 50 kilometers from railway tracks that provide unhindered transportation of equipment and personnel.

In addition, an important criterion is the accessibility of areas with significant settlements. This approach makes it easier to install wind turbines in close nearness to populated areas, resulting in cost savings and reduced energy losses associated with long transmission lines. At the next stage, the selection process is narrowed down to identifying cities and villages with a population exceeding ten thousand inhabitants. This population threshold is chosen because of its demographic significance, as it guarantees a sustainable market for wind energy production. This promotes economic viability, improves network availability and ensures a stable customer base for the project. In addition, such urban centers are more likely to have the necessary infrastructure and resources to support the installation and maintenance of wind energy facilities. Finally, all locations filtered with the stages above will be considered in for the further investigation.

3.7. Multiattribute utility function construction

The decision-making process is a method of collecting data, analyzing options, and choosing an optimal course of action. In the decision analysis (DA) literature and its extension multi attribute utility theory (MAUT) if there is a set of attributes in the problem, the function is considered multiattribute [76]. The most important aspect of MAUT decision analysis

methodology is constructing a multiattribute utility function [77]. Moreover, the most important step in decision analysis (DA) is to accurately represent the true preferences of the decision maker (DM) [51]. In the research, Abbas, 2010 argues that in a case where decision making is non deterministic, each alternative can lead to multiple possible prospects [51]. In instances of decision making under uncertainty, the necessity arises for constructing a von Neumann-Morgenstern utility function, as delineated by the expected utility theory formulated by John von Neumann and Oskar Morgenstern in 1947 [51], [78]. In this situation, MUF can offer a comprehensive mathematical description of the decision maker's preferences for making decisions in a variety of problems [79].

To assess DM preferences, the utility dependence between the attributes must be determined [79], [80], [81]. The utility dependence between alternatives can be described in matrix form or utility dependence matrix (UDM), some cases of UDMs for two attributes are shown in Figure 6. Case (a) asserts that the preference of a DM is utility independent (UI) over two attributes. Which makes the attributes mutually UI [81], meaning MUF can be simplified into *multilinear* form [80], [81], which is detailed in the Equation (22). In Case (b), it is evident that the decision maker's preferences for X_1 remain unaffected by the presence of X_2, and this pattern is mirrored in Case (c) where the preferences are similarly independent of the counterpart variable, making this attributes partial utility independent (PUI) [71]. Finally, Case (d) represents a fully dependent utility matrix preference of DM.

There are several methods that construct a multiattribute utility function [82]. In this research the MUF will be constructed by the method that was established by Keeney and Raiffa [80], because the assessed preferences showed mutual UI between the attributes. The multilinear form of MUF can be applied if every attribute is UI of its complement [80], [81], [82].

	X_1	X_2
X_1	o	
X_2		o

(a)

	X_1	X_2
X_1	o	
X_2	o	o

(b)

	X_1	X_2
X_1	o	o
X_2		o

(c)

	X_1	X_2
X_1	o	o
X_2	o	o

(d)

Figure 6. Utility dependency matrices (UDMs), four cases for two attributes, (a) mutually utility independent (MUI) identity matrix, (b) and (c) partially utility independent (PUI)

***matrixes, (d) fully dependent matrix. Source: Adapted from* [82].**

The following equation describes the multilinear form [80]:

$$\begin{aligned} &\sum_{i=1}^{n} k_i u_i(x_i) + \sum\sum_{i>j} k_{ij} u_i(x_i) u_j(x_j) + \cdots + k_{123\ldots n} u_1(x_1) u_2(x_2) \ldots u_n(x_n) \quad (22) \\ &u(x_1, \ldots, x_n) = \sum_{i=1}^{n} k_i \end{aligned}$$

where lowercase letters x_i denote the instantiation of attribute X_i, $u_i(x_i)$ is the one attribute utility function of X_i, and scaling constants k_i which are equal to $k_i = u_i(x_i^*, x_i^0)$, and $k_{ij} = 1 - k_i - k_j$, the x_i^*- the best possible outcome instantiation, and x_i^0- the worst possible outcome instantiation of attribute X_i.

For graphical representation of alternatives and attributes with expected utility, i.e. von Neumann-Morgenstern utility function, an expected utility tree or decision tree needs to be constructed [77] as shown in Figure 7. This representation allows to display the decision sequence and identify the utility of each alternative. The option with the highest expected utility will have the best outcome after evaluating the utility of each alternative. In order to derive the expected utility for each option (i.e. alternative), the initial step involves determining the values for each attribute: high, base, and low values in Decision Tree Figure 7. These values are derived from the distribution functions. For instance, for attribute X_1 Potential power output, the calculation employs the Weibull distribution, Equation (1). For X_2, which relates to GHG emission reduction potential, the Gaussian distribution is utilized, Equation (18). This process enables the determination of high, base, and low values. It is possible to obtain a utility function using a single attribute, $u_i(x_i)$, after assessing the decision maker's genuine preferences. Additionally, once a comparable procedure of evaluating preferences for multiple attributes has been completed, the multiattribute utility function can be determined.

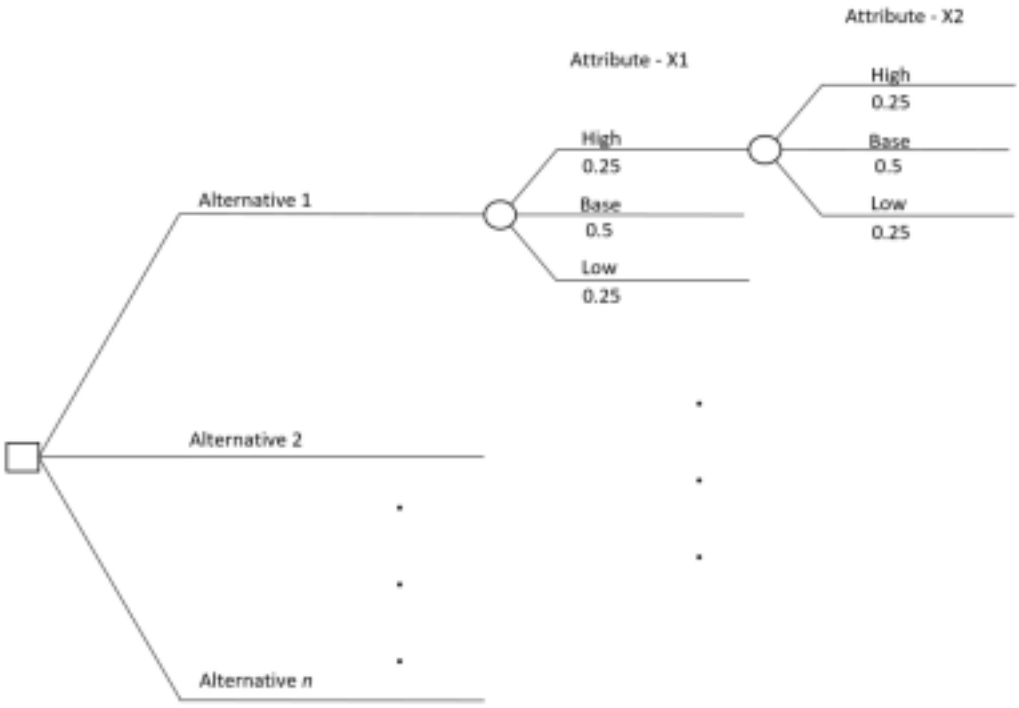

Figure 7. Simplified Decision Tree (DT). Source: Author development.

Chapter 4 – Results

Initially, potential research sites that met the specified requirements were identified. Subsequently, statistical characteristics related to wind energy production potential – X_1 and greenhouse gas emission reduction potential – X_2 were quantified. This assessment was facilitated by constructing a decision tree and developing a questionnaire for a Decision Maker (DM) to obtain the preferences. Answers of the questionnaire allowed to determinate the expected utility E(U) for X_1 and X_2. The final step in this process was the refinement mathematical model of the multiattribute utility function (MUF).

In this study, the selection of study sites and the creation of wind speed maps in Kazakhstan were performed using QGIS 3.32.3. Mapping data was obtained from [83], [84], [85] and wind speed hourly data for twenty specific locations from 01/01/2019 to 31/12/2023 was obtained from database of NASA's modern-era retrospective analysis for research and applications version 2 (MERRA-2) [86], [87], [88]. Calculations of attribute values and subsequent decision-making process using MUF were performed using PyCharm version 2022.3.1. The following subsections discuss the application of the methodology and demonstrate the results of this study, which are important for improving the understanding of wind energy decision-making processes and strategies for reducing greenhouse gas emissions in Kazakhstan.

4.1. Location selection

Locations were chosen based on criteria suitable for efficient wind energy generation discussed in methodology section. Mapping data for Kazakhstan was obtained from the resources [83], [84], [85], and it was processed using the QGIS program version 3.32.3.

Initially based on the analysis of the road infrastructure of Kazakhstan, 223 cities and towns were identified. These cities were strategically located within a radius of 5–10 kilometers from highways and at least 50 kilometers from railways. This selection was made to ensure efficient energy transfer and minimize losses in long transmission lines. After this, 113 cities and towns were specially selected, each of which has more than ten thousand inhabitants. This selection was aimed at meeting the criteria set by the IEC for the classification of wind turbines [75]. Of these

113 locations, 20 were identified that not only met the above requirements, but also exhibited an optimal wind speed at the height of 50 meters above ground level. Figure 8 illustrate a map of selected locations with the requirements listed, and Table 2 represents a locations' annual mean wind speed at 50 m and 100 m heights, and the coordinates, the names of the locations are the nearest cities to the point in the map. Appendixes A – D demonstrate the detailed mapping of Kazakhstan with highways and railways, cities, as well as wind speeds at the height of 50 and 100 meters.

Figure 8. Map of selected locations in Kazakhstan.

Table 2: Characteristics of Selected locations. Sources: **[84], [85], [87].**

№ Alternatives	***Coordinates (latitude , longitude)***	***Average mean wind speed (m/s) at 50 m***	***Average mean wind speed (m/s) at 100 m***
1	*3,87*		
Dzungarian Gate	*45.35, 82.45*	*3,51*	
Shelek	*43.73, 78.26*	*4,88*	
Fort-Shevchenko	*44.49, 50.29*	*7,52*	
Arkalyk	*50.07, 66.73*	*7,32*	
Yereymentau	*51.59, 73.15*	*7,35*	
Karkaralinsk	*48.84, 79.19*	*6,46*	
Janatas	*43.47, 69.67*	*7,25*	
Emba	*48.73, 58.48*	*6,99*	
Along Caspian sea	*46.38, 53.12*	*7,05*	

Atbasar	*51.77, 68.41*	*7,00*
Zaysan	*48.01, 84.68*	*5,42*
Kyzylorda	*44.94, 65.91*	*7,03*
Baikonur	*45.53, 63.48*	*6,96*
Beyneu	*45.13, 54.98*	*6,90*

2 *5,38* 3 *8,29* 4 *8,06* 5 *8,10* 6 *7,12* 7 *7,99* 8 *7,71* 9 *7,77* 10 *7,72* 11 *5,97* 12 *7,75* 13 *7,67* 14 *7,60*
15 Shetpe *44.15, 52.09 7,17 7,90*

16 Zhanaozen *43.41, 52.87 6,95 7,66* 17 *7,88*

Zhetibay	*43.54, 52.03*	*7,15*
Eski Ikan	*43.23, 69.21*	*6,91*
Georgievka	*49.14, 81.73*	*6,26*

18 *7,61* 19 *6,90* 20 Ulbi *50.25, 83.46 4,51 4,97*

4.2. Wind turbine selection

The wind turbine selection is the next step in the wind power plant installation projects [74]. Choosing the appropriate wind turbine is essential in the effective implementation of wind power plant projects. In this study, two distinct wind turbine models, the Vestas V52 and Vestas V90, were chosen, with hub heights of 50 and 100 meters, respectively. These turbine models were selected based on their specific characteristics, which are presented in Table 3. Notably, the main characteristic under consideration is the rated power, with values of 850 kW and 2000 kW for the Vestas V52 and Vestas V90 models, respectively. The comparison of the power curves of two selected wind turbine models are shown in Figure 9.

Table 3: Characteristics of selected Wind Turbines for hub height at 50 and 100 meters. Sources: **[89], [90].**

Characteristics Vestas V90 Vestas V52

Vestas
V90-2.0 MW
2000 kW
100 m
45 m
3
6362 m²
4 m/s

Wind Turbine Manufacturer Vestas Wind turbine model *V52-850 kW* Rated power, kW *850 kW* Hub height, m *50 m* Blade length, m *26 m* Number of blades, qnt. *3* Swept area, m² *2124 m²* Cut-in wind speed, m/s *4 m/s* Cut-out wind speed, m/s *25 m/s 25 m/s*

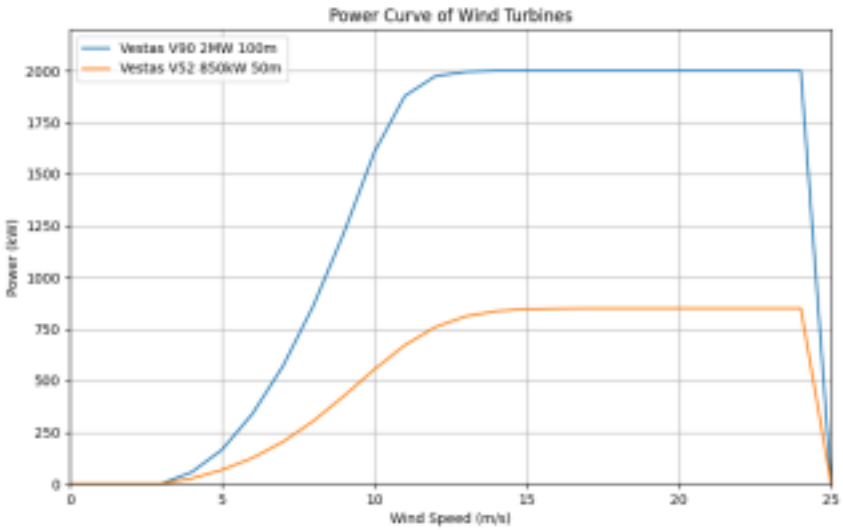

Figure 9. Power curve comparison. Source: Adapted from [89], [90].

4.3. Calculation of attributes X_1 and X_2

This subsection will provide the analysis of wind speed data for potentially efficient locations in Kazakhstan, and also provide the analysis of data for potential reductions in greenhouse gas emissions, and their statistical normalized data for the further multiattribute utility function construction.

4.3.1. X_1 Potential power output

In approximating the wind speed data at the desired hub height, Wind shear Equation (12) was applied, where the WSE α, representing the coefficient influenced by the topography at the site. The data of mean monthly speed at 50 and 100 meters presented in the Table 3. The data demonstrate a pattern across all selected sites, the high wind speeds tend to occur during the winter autumn seasons, whereas the low wind speeds are observed during the summer-spring seasons. This trend underscores the seasonal variability of wind patterns and highlights the importance of considering seasonal fluctuations in wind speed when assessing wind energy potential.

***Table 3: Mean monthly wind speed (m/s) in selected locations. Sources:* [86], [87], [88].**

Dzungarian Gate		*Shelek Fort-Shevchenko*		*Arkalyk*		
50 m	*100 m*	*50 m*	*100 m*	*50 m*	*100 m*	*50 m*
2,94	*3,24*	*4,87*	*5,36*	*8,32*	*9,17*	*7,69*
2,80	*3,09*	*4,70*	*5,18*	*7,32*	*8,07*	*7,62*
3,29	*3,62*	*4,90*	*5,40*	*7,77*	*8,56*	*8,22*
3,96	*4,36*	*4,68*	*5,16*	*7,49*	*8,26*	*7,57*
4,51	*4,97*	*4,90*	*5,40*	*7,25*	*7,99*	*6,91*

4,25	*4,68*	*4,52*	*4,98*	*6,66*	*7,33*	*6,54*
4,07	*4,48*	*4,59*	*5,06*	*6,79*	*7,49*	*6,46*
3,66	*4,03*	*4,48*	*4,94*	*6,40*	*7,05*	*6,67*
3,51	*3,87*	*4,82*	*5,31*	*6,44*	*7,10*	*6,59*
3,28	*3,62*	*4,91*	*5,41*	*6,79*	*7,48*	*6,99*
3,32	*3,66*	*4,85*	*5,34*	*6,67*	*7,35*	*6,99*

Height *100 m* January *8,47* February *8,39* March *9,05* April *8,34* May *7,61* June *7,21* July *7,12* August *7,35* September *7,26* October *7,71* November *7,70* December *3,18 3,51 5,20 5,73 8,19 9,02 7,88 8,68*

Karkaralinsk Janatas Emba Caspian sea

50 m	*100 m*	*50 m*	*100 m*	*50 m*	*100 m*	*50 m*
6,86	*7,56*	*6,92*	*7,62*	*7,23*	*7,97*	*7,59*
6,53	*7,20*	*6,74*	*7,42*	*7,06*	*7,78*	*6,94*
6,55	*7,21*	*6,96*	*7,66*	*7,46*	*8,22*	*7,64*
6,27	*6,91*	*6,86*	*7,56*	*7,23*	*7,97*	*7,55*
6,21	*6,85*	*7,45*	*8,21*	*7,13*	*7,86*	*7,16*
5,53	*6,09*	*6,77*	*7,46*	*6,74*	*7,42*	*6,69*
5,95	*6,56*	*7,10*	*7,83*	*6,42*	*7,08*	*6,30*
5,63	*6,21*	*7,28*	*8,03*	*6,56*	*7,22*	*6,27*
5,85	*6,45*	*7,20*	*7,93*	*6,33*	*6,97*	*5,99*
6,48	*7,14*	*7,79*	*8,59*	*6,58*	*7,25*	*6,54*
6,32	*6,97*	*7,77*	*8,56*	*6,54*	*7,21*	*6,51*
7,34	*8,09*	*7,60*	*8,38*	*7,44*	*8,20*	*7,58*
Zaysan		***Kyzylorda***		***Baikonur***		***Beyn***
50 m	*100 m*	*50 m*	*100 m*	*50 m*	*100 m*	*50 m*
5,46	*6,02*	*6,70*	*7,38*	*6,63*	*7,31*	*7,16*
5,24	*5,77*	*7,01*	*7,72*	*6,83*	*7,53*	*6,84*

5,58	*6,15*	*6,95*	*7,66*	*6,94*	*7,65*	*7,30*
5,39	*5,94*	*7,32*	*8,06*	*7,41*	*8,17*	*7,15*
5,55	*6,12*	*7,44*	*8,20*	*7,38*	*8,13*	*6,81*
5,24	*5,77*	*6,65*	*7,33*	*6,63*	*7,30*	*6,39*
4,88	*5,37*	*6,58*	*7,25*	*6,52*	*7,18*	*6,31*
4,63	*5,10*	*6,59*	*7,26*	*6,55*	*7,22*	*6,42*
4,83	*5,32*	*6,76*	*7,45*	*6,85*	*7,55*	*6,31*

Height (m) *100 m* January *8,36* February *7,65* March *8,42* April *8,31* May *7,89* June *7,37* July *6,95* August *6,91* September *6,60* October *7,21* November *7,17* December *8,35*

Height (m) *100 m* January *7,89* February *7,53* March *8,04* April *7,87* May *7,50* June *7,04* July *6,95* August *7,07* September *6,95* October *5,16 5,68 7,13 7,85 6,92 7,63 6,72 7,40*

November *5,06 5,58 7,12 7,84 6,91 7,61 6,58 7,25*

5,93	*6,54*	*7,21*	*7,94*	*7,09*	*7,81*	*7,30*
Zhanaozen		***Zhetibay***		***Eski Ikan***		
50 m	*100 m*	*50 m*	*100 m*	*50 m*	*100 m*	*50 m*
7,17	*7,90*	*7,48*	*8,25*	*6,39*	*7,04*	*7,24*
6,48	*7,14*	*6,74*	*7,43*	*5,99*	*6,60*	*7,31*
7,05	*7,77*	*7,17*	*7,90*	*6,34*	*6,98*	*6,85*
7,11	*7,84*	*7,20*	*7,94*	*6,58*	*7,25*	*6,27*
6,69	*7,38*	*6,72*	*7,41*	*6,99*	*7,70*	*6,35*
6,46	*7,12*	*6,39*	*7,04*	*6,47*	*7,13*	*5,48*
6,40	*7,05*	*6,53*	*7,19*	*7,05*	*7,77*	*5,55*
6,38	*7,04*	*6,30*	*6,94*	*7,29*	*8,03*	*5,05*
6,56	*7,23*	*6,65*	*7,33*	*7,38*	*8,13*	*4,97*
6,91	*7,61*	*7,09*	*7,81*	*7,89*	*8,69*	*5,60*

6,85	*7,55*	*7,05*	*7,77*	*7,84*	*8,64*	*5,44*

December *8,05* ***Georgievka***

Height (m) *100 m* January *7,97* February *8,06* March *7,54* April *6,91* May *6,99* June *6,04* July *6,12* August *5,57* September *5,47* October *6,17* November *6,00* December *7,47 8,23 7,79 8,58 7,24 7,98 6,78 7,47*

Yereymentau Atbasar Shetpe Ubli

50 m	*100 m*	*50 m*	*100 m*	*50 m*	*100 m*	*50 m*
8,48	*9,34*	*7,12*	*7,85*	*7,42*	*8,18*	*5,19*
8,06	*8,88*	*7,12*	*7,85*	*6,78*	*7,47*	*4,81*
8,60	*9,47*	*7,99*	*8,80*	*7,29*	*8,03*	*5,02*
7,54	*8,31*	*7,24*	*7,98*	*7,36*	*8,11*	*4,37*
6,49	*7,16*	*6,61*	*7,28*	*6,93*	*7,64*	*4,33*
6,27	*6,91*	*6,52*	*7,18*	*6,63*	*7,31*	*3,87*
6,24	*6,88*	*6,21*	*6,84*	*6,63*	*7,30*	*3,77*
6,25	*6,89*	*6,46*	*7,12*	*6,42*	*7,07*	*3,75*
5,91	*6,51*	*6,48*	*7,14*	*6,68*	*7,36*	*3,76*
6,52	*7,19*	*6,50*	*7,17*	*6,98*	*7,69*	*4,17*
6,48	*7,14*	*6,50*	*7,16*	*6,96*	*7,67*	*4,12*

Height (m) *100 m* January *5,72* February *5,30* March *5,54* April *4,81* May *4,77* June *4,27* July *4,16* August *4,13* September *4,14* October *4,59* November *4,54* December *8,47 9,34 7,67 8,45 7,72 8,50 5,20 5,73*

To describe wind speed variability, the Weibull two-parameter function utilized. The calculated probability and cumulative density functions, Equations (1 – 2) for the shape and scale parameters *k* and *c* among the studied locations are presented in Table 4. The Weibull parameters were estimated using Energy pattern factor method Equations (3 – 5). The plots of Weibull probability and cumulative density functions, comparing with the observed data for all sites are detailed in Appendix I and J.

Table 4: Weibull parameters of selected locations at 50 and 100 meters height. **№ Alternatives** ***h = 50 m h = 100 m*** ***F(V)***

	V	*k*	*c*	*f(V)*	*F(V)*	*V*	*k*	*c*	*f(V)*
Dzungarian Gate	*3,51*	*1,97*	*3,96*	*0,20*	*0,55*	*3,87*	*1,97*	*4,36*	*0,18*
Shelek	*4,88*	*2,84*	*5,48*	*0,20*	*0,51*	*5,38*	*2,84*	*6,03*	*0,19*
Fort-Shevchenko	*7,52*	*2,56*	*8,47*	*0,12*	*0,52*	*8,29*	*2,56*	*9,34*	*0,11*
Arkalyk	*7,32*	*2,70*	*8,23*	*0,13*	*0,52*	*8,06*	*2,70*	*9,07*	*0,12*
Yereymentau	*7,35*	*2,52*	*8,28*	*0,12*	*0,52*	*8,10*	*2,52*	*9,12*	*0,11*
Karkaralinsk	*6,46*	*2,47*	*7,29*	*0,14*	*0,52*	*7,12*	*2,47*	*8,03*	*0,12*
Janatas	*7,25*	*2,59*	*8,16*	*0,13*	*0,52*	*7,99*	*2,59*	*8,99*	*0,11*
Emba	*6,99*	*2,87*	*7,85*	*0,14*	*0,51*	*7,71*	*2,87*	*8,65*	*0,13*
Along Caspian sea	*7,05*	*2,78*	*7,92*	*0,14*	*0,52*	*7,77*	*2,78*	*8,73*	*0,13*
Atbasar	*7,00*	*2,74*	*7,87*	*0,14*	*0,52*	*7,72*	*2,74*	*8,67*	*0,12*
Zaysan	*5,42*	*2,39*	*6,12*	*0,16*	*0,53*	*5,97*	*2,39*	*6,74*	*0,14*
Kyzylorda	*7,03*	*2,96*	*7,88*	*0,15*	*0,51*	*7,75*	*2,96*	*8,68*	*0,13*
Baikonur	*6,96*	*3,02*	*7,80*	*0,15*	*0,51*	*7,67*	*3,02*	*8,59*	*0,14*
Beyneu	*6,90*	*2,80*	*7,75*	*0,14*	*0,51*	*7,60*	*2,80*	*8,54*	*0,13*
Shetpe	*7,17*	*2,91*	*8,04*	*0,14*	*0,51*	*7,90*	*2,91*	*8,86*	*0,13*
Zhanaozen	*6,95*	*2,91*	*7,80*	*0,15*	*0,51*	*7,66*	*2,91*	*8,59*	*0,13*
Zhetibay	*7,15*	*2,88*	*8,02*	*0,14*	*0,51*	*7,88*	*2,88*	*8,84*	*0,13*
Eski Ikan	*6,91*	*2,48*	*7,79*	*0,13*	*0,52*	*7,61*	*2,48*	*8,58*	*0,11*
Georgievka	*6,26*	*2,65*	*7,05*	*0,15*	*0,52*	*6,90*	*2,65*	*7,77*	*0,14*

1 *0,55* 2 *0,51* 3 *0,52* 4 *0,52* 5 *0,52* 6 *0,52* 7 *0,52* 8 *0,51* 9 *0,52* 10 *0,52* 11 *0,53* 12 *0,51* 13 *0,51* 14 *0,51* 15 *0,51*

16 *0,51* 17 *0,51* 18 *0,52* 19 *0,52* 20 Ulbi *4,51 2,36 5,09 0,18 0,53 4,97 2,36 5,61 0,17 0,53*

To calculate the average annual power density (W/m^2) values, Equation (8) was used. The results were computed for the designated sites and are presented in Table 5. According to the NREL wind classification most of the selected locations in Kazakhstan has 3 classification at 50 m height and 4 classification at 100 m [91].

Table 5: Annual mean power density in selected locations.

№ Alternatives ***Annual mean power density (W/m²)***

		Yereymentau	*382,56*
Dzungarian Gate		Karkaralinsk	*248,05*
Shelek		Janatas	*344,30*
Fort-Shevchenko			
Arkalyk			

h = 100m

1 *63,95* 2 *126,86* 3 *544,80* 4 *476,74* 5 *509,28* 6 *330,20* 7 *458,40* 8 Emba *299,81 399,14*

9 Along Caspian sea *320,38 426,55* 10 *417,63*

Atbasar	*313,72*
Zaysan	*141,93*
Kyzylorda	*301,11*
Baikonur	*291,11*
Beyneu	*296,52*
Shetpe	*321,79*
Zhanaozen	*291,84*
Zhetibay	*319,42*
Eski Ikan	*308,01*
Georgievka	*220,66*

11 *188,94* 12 *400,90* 13 *387,58* 14 *394,79* 15 *428,44* 16 *388,57* 17 *425,29* 18 *410,08* 19 *293,75* 20 Ulbi *84,23 112,12*

An additional investigation of the efficiency of obtaining the parameters *k* and *c* was conducted in order to evaluate the efficacy of the method for estimating the Weibull parameters *Epf*. The most effective technique for estimating the parameters is determined by utilizing a number of statistics to assess the effectiveness of estimation techniques. For wind data analysis, R^2, and RMSE are commonly used metrics Equations (13 – 14). The results of statistical test of EPFM method presented in Table 6.

Table 6: Performance test on EPFM method, estimation of Weibull parameters. **№**

Alternatives ***RMSE R^2 100 meters***

	50 meters	***100 meters***	***50 meters***
Dzungarian Gate	*0,039289*	*0,03637*	*0,776869*
Shelek	*0,02891*	*0,026398*	*0,888324*
Fort-Shevchenko	*0,009805*	*0,009668*	*0,957659*
Arkalyk	*0,0115*	*0,011217*	*0,968361*
Yereymentau	*0,010793*	*0,010551*	*0,969879*
Karkaralinsk	*0,013363*	*0,012381*	*0,959224*
Janatas	*0,010549*	*0,009423*	*0,971378*
Emba	*0,010106*	*0,009182*	*0,976524*
Along Caspian sea	*0,009464*	*0,00925*	*0,978763*
Atbasar	*0,012251*	*0,011779*	*0,966275*
Zaysan	*0,012447*	*0,012135*	*0,967956*
Kyzylorda	*0,01184*	*0,010416*	*0,955398*
Baikonur	*0,013305*	*0,01119*	*0,963639*
Beyneu	*0,010859*	*0,0102*	*0,973353*
Shetpe	*0,011486*	*0,011072*	*0,970595*

1 *0,783545* 2 *0,897155* 3 *0,952386* 4 *0,966902* 5 *0,968529* 6 *0,961419* 7 *0,974761* 8 *0,978672* 9 *0,977787* 10 *0,96575* 11 *0,966658* 12 *0,960112* 13 *0,971463* 14 *0,974149* 15 *0,970101* 16 Zhanaozen *0,010819 0,01038 0,974317 0,974138*

17 Zhetibay *0,012935 0,01252 0,962724 0,961679*

Eski Ikan	*0,014008*	*0,011859*	*0,951692*
Georgievka	*0,012562*	*0,012802*	*0,966057*

18 *0,961434* 19 *0,961622* 20 Ulbi *0,023514 0,022262 0,913015 0,914373*

From the Table 6 it is clear that EPFM method is accurate in estimating the *k* and *c* parameters of hourly wind speed data at 50 and 100 meters. The potential power output of attribute X_1 has been determined through the application of Equation (9). To calculate the capacity factor Equation (10) was used. In this particular analysis, the losses coefficient remained constant for all locations Equation (11), accounting for 5% array losses, 5% downtime losses, 5% miscellaneous losses, and 5% airfoil losses, which is average values for the initial guess [64]. The outcomes for P_{out} (MWh/year) and C_f (%) are detailed in Table 7.

The determination of potential power output (X_1 attribute) and capacity factor at twenty locations in Kazakhstan was successfully done. The findings highlight that sites such as Fort Shevchenko, Yereymentau, Arkalyk, Janatas, Zhetibay, Shetpe, and those along the Caspian Sea exhibit the highest power output at each hub height. The wind power density was analyzed, revealing a class 3 at a height of 50 meters and class 4 at an height of 100 meters based on established wind criteria by NREL [91]. Additionally, the results of the Weibull PDFs and CDFs functions calculations were obtained. These outcomes were subjected to a statistical test, confirming a highly accurate estimation of the parameters.

Within the MAUT methodology, and application of the statistical analysis, it is first necessary to extract the values of the first attribute, potential power output X_1. Minimum, low, base, high, and maximum values are extracted for further examination. Table 8 presents the data for the aforementioned statistical values of a wind speed, pressure, temperature, air density, and

power output at each site, and also the constant values of swept area for each turbine and constant capacity factor for each location. The wind speed distribution was modeled using the Weibull CDF Equation (2), while the temperature and pressure distributions were represented by the Gaussian normal distribution CDF, Equation (19). Additionally, Appendix I provides CDF plots of a wind speed for each site, illustrating the distribution of values corresponding to the minimum, low, base, high, and maximum.

Table 7 : Annual potential power output (MWh/year) and capacity factor (%) for different wind turbines: VESTAS V52 – 850 kW – 50 m and VESTAS V90 – 2 MW – 100 m (calculated for one wind turbine installed).

Wind turbine *VESTAS V52 – 0.85 MW – 50 m VESTAS V90 –2.0 MW – 100 m*

Alternatives	P_{out} ***(MWh/year)***	C_f ***(%)***	P_{out} ***(MWh/year)***
Dzungarian Gate	*81,34*	*18%*	*463,74*
Shelek	*136,49*	*11%*	*811,07*
Fort-Shevchenko	*1 525,80*	*31%*	*7 885,36*
Arkalyk	*1 309,38*	*29%*	*7 165,18*
Yereymentau	*1 351,79*	*30%*	*7 305,98*
Karkaralinsk	*669,62*	*23%*	*3 704,11*
Janatas	*1 213,65*	*29%*	*6 546,74*
Emba	*1 048,55*	*27%*	*5 866,03*
Along Caspian sea	*1 126,05*	*28%*	*6 243,48*
Atbasar	*1 048,75*	*27%*	*5 855,98*
Zaysan	*261,40*	*16%*	*1 508,60*
Kyzylorda	*1 073,46*	*27%*	*6 063,85*
Baikonur	*1 020,71*	*26%*	*5 823,07*
Beyneu	*981,09*	*26%*	*5 507,73*
Shetpe	*1 182,69*	*28%*	*6 563,05*

Zhanaozen	*1 003,56*	*26%*	*5 635,22*
Zhetibay	*1 165,27*	*28%*	*6 420,28*
Eski Ikan	*980,06*	*27%*	*5 297,50*
Georgievka	*629,71*	*23%*	*3 515,93*

№ C_f (%) 1 *25%* 2 *17%* 3 *40%* 4 *40%* 5 *40%* 6 *32%* 7 *39%* 8 *38%* 9 *39%* 10 *37%* 11 *23%* 12 *38%* 13 *38%* 14 *37%* 15 *39%* 16 *37%* 17 *39%* 18 *37%* 19 *33%* 20 Ulbi *92,34 10% 553,38 15%*

Table 8 : X_1 attribute – Potential power output. Min, low, base, high, and max values for wind speed, pressure, temperature, air density, blade swept area, capacity factor, and power output in each site at 50 and 100 meters height.

Dzungarian Gate h = 50 meters h = 100 meters

Unit	*Min*	*Low*	*Base*	*High*	*Max*	*Min*	*Low*	*Base*	*High*
m/s	*0*	*1,28*	*3,32*	*6,09*	*25*	*0*	*1,4*	*3,64*	*6,69*
°C	*-28,025*	*-13,09*	*-0,53*	*12,04*	*17,905*	*-28,35*	*-13,42*	*-0,85*	*11,71*
kPa	*70,46*	*71,33*	*71,78*	*72,22*	*72,74*	*70,00*	*70,88*	*71,33*	*71,78*
kg/m^3	*0,8707*	*0,8822*	*0,9173*	*0,9555*	*1,0014*	*0,8661*	*0,8778*	*0,9126*	*0,9507*

Variables Max Wind speed *25* Temperature *17,58* Pressure *72,28* Air density *0,9961* Blade swept area - *const*$^{m^2}$ *2123,72 2123,72 2123,72 2123,72 2123,72 6362 6362 6362 6362 6362*

Capacity factor - *const*$^{\%}$ *17,7% 17,7% 17,7% 17,7% 17,7% 25,2% 25,2% 25,2% 25,2% 25,2%* Power output *MWh/year* ***0,000 3,039 55,140 354,534 25703,988 0,000 16,945 309,601 2002,410 109488,050***

Shelek

Variables Unit Min Low Base High Max Min Low Base High Max

m/s	*0*	*2,48*	*4,84*	*7,37*	*19,62*	*0*	*2,76*	*5,33*	*8,13*
°C	*-19,315*	*-3,47*	*9,82*	*23,1*	*31,185*	*-19,64*	*-3,79*	*9,49*	*22,78*
kPa	*86,95*	*87,74*	*88,37*	*89,00*	*90,20*	*86,41*	*87,22*	*87,84*	*88,45*

kg/m³	*1,0325*	*1,0466*	*1,0879*	*1,1334*	*1,1933*	*1,0267*	*1,0412*	*1,0827*	*1,1280*
m²	*2123,72*	*2123,72*	*2123,72*	*2123,72*	*2123,72*	*6362*	*6362*	*6362*	*6362*
%	*11,2%*	*11,2%*	*11,2%*	*11,2%*	*11,2%*	*16,6%*	*16,6%*	*16,6%*	*16,6%*

Wind speed *21,62* Temperature *30,86* Pressure *89,59* Air density *1,1874* Blade swept area - $const^{6362}$ Capacity factor - $const^{16,6\%}$ Power output *MWh/year* ***0,000 16,577 128,092 471,164 9358,779 0,000 101,462 759,817 2809,461 55613,636***

Fort-Shevchenko

Variables Unit Min Low Base High Max Min Low Base High Max

m/s	*0*	*3,52*	*7,37*	*11,77*	*25*	*0*	*3,88*	*8,13*	*12,97*
°C	*-12,135*	*0,84*	*12,81*	*24,78*	*30,705*	*-12,46*	*0,52*	*12,49*	*24,46*
kPa	*98,88*	*100,37*	*101,39*	*102,40*	*104,50*	*98,28*	*99,79*	*100,78*	*101,77*
kg/m³	*1,1981*	*1,1974*	*1,2352*	*1,2762*	*1,3198*	*1,1917*	*1,1913*	*1,2291*	*1,2703*
m²	*2123,72*	*2123,72*	*2123,72*	*2123,72*	*2123,72*	*6362*	*6362*	*6362*	*6362*
%	*31,1%*	*31,1%*	*31,1%*	*31,1%*	*31,1%*	*40,3%*	*40,3%*	*40,3%*	*40,3%*

Wind speed *25* Temperature *30,38* Pressure *103,83* Air density *1,3133* Blade swept area - $const^{6362}$ Capacity factor - $const^{40,3\%}$ Power output *MWh/year* ***0,000 151,209 1431,719 6025,096 59708,697 0,000 782,052 7423,268 31149,275 230628,803***

Arkalyk

Variables Unit Min Low Base High Max Min Low Base High Max

m/s	*0*	*3,6*	*7,21*	*11,21*	*25*	*0*	*3,96*	*7,93*	*12,37*
°C	*-31,385*	*-13,84*	*4,63*	*23,11*	*33,645*	*-31,71*	*-14,17*	*4,31*	*22,78*
kPa	*94,17*	*95,89*	*97,05*	*98,20*	*99,66*	*93,58*	*95,32*	*96,45*	*97,58*
kg/m³	*1,1316*	*1,1547*	*1,2171*	*1,2882*	*1,3569*	*1,1256*	*1,1487*	*1,2110*	*1,2822*
m²	*2123,72*	*2123,72*	*2123,72*	*2123,72*	*2123,72*	*6362*	*6362*	*6362*	*6362*
%	*29,4%*	*29,4%*	*29,4%*	*29,4%*	*29,4%*	*40,4%*	*40,4%*	*40,4%*	*40,4%*

Wind speed *25* Temperature *33,32* Pressure *99,02* Air density *1,3502* Blade swept

area - $const^{6362}$ Capacity

factor - $const^{40,4\%}$ Power output *MWh/year* ***0,000 147,402 1248,121 4965,090 58008,045 0,000 802,257 6791,688 27295,006 237271,959***

Yereymentau

Variables Unit Min Low Base High Max Min Low Base High Max Wind speed *m/s 0 3,4 7,17 11,53 25 0 3,76 7,93 12,73 25*

Temperature *°C -34,205 -15,65 2,53 20,71 30,725 -34,53 -15,98 2,2 20,38 30,4*

kPa	*94,08*	*95,56*	*96,71*	*97,87*	*99,71*	*93,54*	*94,99*	*96,11*	*97,24*
kg/m^3	*1,1431*	*1,1602*	*1,2221*	*1,2928*	*1,3716*	*1,1363*	*1,1541*	*1,2160*	*1,2868*
m^2	*2123,72*	*2123,72*	*2123,72*	*2123,72*	*2123,72*	*6362*	*6362*	*6362*	*6362*
%	*29,8%*	*29,8%*	*29,8%*	*29,8%*	*29,8%*	*40,3%*	*40,3%*	*40,3%*	*40,3%*

Pressure *99,01* Air density *1,3656* Blade swept

area - $const^{6362}$ Capacity

factor - $const^{40,3\%}$ Power output *MWh/year* ***0,000 126,288 1247,499 5487,866 59350,997 0,000 689,750 6817,718 29845,495 239905,050***

Karkaralinsk

Variables Unit Min Low Base High Max Min Low Base High Max

m/s	*0*	*2,96*	*6,29*	*10,25*	*25*	*0*	*3,24*	*6,93*	*11,29*
°C	*-32,255*	*-13,71*	*3,82*	*21,34*	*29,235*	*-32,58*	*-14,03*	*3,49*	*21,01*
kPa	*92,00*	*92,88*	*93,85*	*94,83*	*96,39*	*91,48*	*92,34*	*93,27*	*94,21*
kg/m^3	*1,1105*	*1,1218*	*1,1804*	*1,2472*	*1,3304*	*1,1039*	*1,1157*	*1,1745*	*1,2415*
m^2	*2123,72*	*2123,72*	*2123,72*	*2123,72*	*2123,72*	*6362*	*6362*	*6362*	*6362*
%	*23,1%*	*23,1%*	*23,1%*	*23,1%*	*23,1%*	*32,0%*	*32,0%*	*32,0%*	*32,0%*

Wind speed *25* Temperature *28,91* Pressure *95,71* Air density *1,3247* Blade swept

area - $const^{6362}$ Capacity

factor - $const^{32,0\%}$ Power output *MWh/year* ***0,000 62,514 631,216 2885,903 44667,204 0,000 338,827 3490,253 15951,478 184803,936***

Janatas

Variables Unit Min Low Base High Max Min Low Base High Max

m/s	*0*	*3,44*	*7,09*	*11,29*	*25*	*0*	*3,8*	*7,81*	*12,41*

°C	*-22,825*	*-5,68*	*10,19*	*26,07*	*33,825*	*-23,15*	*-6*	*9,87*	*25,74*
kPa	*92,65*	*93,30*	*94,14*	*94,99*	*96,83*	*92,08*	*92,76*	*93,57*	*94,39*
kg/m³	*1,0988*	*1,1059*	*1,1575*	*1,2152*	*1,2894*	*1,0925*	*1,1002*	*1,1518*	*1,2096*
m²	*2123,72*	*2123,72*	*2123,72*	*2123,72*	*2123,72*	*6362*	*6362*	*6362*	*6362*
%	*29,2%*	*29,2%*	*29,2%*	*29,2%*	*29,2%*	*39,4%*	*39,4%*	*39,4%*	*39,4%*

Wind speed *25* Temperature *33,5* Pressure *96,17* Air density *1,2831* Blade swept area - *const*^{6362} Capacity factor - *const*$^{39,4\%}$ Power output *MWh/year* ***0,000 122,101 1118,824 4742,915 54640,579 0,000 663,355 6029,114 25403,983 220308,223***

Emba

Variables Unit Min Low Base High Max Min Low Base High Max

m/s	*0*	*3,6*	*6,93*	*10,53*	*25*	*0*	*3,96*	*7,65*	*11,57*
°C	*-33,075*	*-11,54*	*7,11*	*25,75*	*33,945*	*-33,4*	*-11,86*	*6,78*	*25,43*
kPa	*95,01*	*96,91*	*98,04*	*99,17*	*101,28*	*94,42*	*96,34*	*97,44*	*98,54*
kg/m³	*1,1490*	*1,1558*	*1,2187*	*1,2905*	*1,3787*	*1,1424*	*1,1497*	*1,2126*	*1,2845*
m²	*2123,72*	*2123,72*	*2123,72*	*2123,72*	*2123,72*	*6362*	*6362*	*6362*	*6362*

Wind speed *25* Temperature *33,62* Pressure *100,60* Air density *1,3720* Blade swept area - *const*^{6362} Capacity

factor - *const*$^{\%\ 27,1\%\ 27,1\%\ 27,1\%\ 27,1\%\ 27,1\%\ 38,0\%\ 38,0\%\ 38,0\%\ 38,0\%\ 38,0\%}$

Power output *MWh/year* ***0,000 135,960 1022,565 3798,815 54313,302 0,000 756,430 5751,796 21077,315 227117,997 Along Caspian sea***

Variables Unit Min Low Base High Max Min Low Base High Max

m/s	*0*	*3,56*	*6,97*	*10,69*	*25*	*0*	*3,92*	*7,69*	*11,81*
°C	*-22,515*	*-6,42*	*10,68*	*27,78*	*35,485*	*-22,84*	*-6,75*	*10,35*	*27,45*
kPa	*98,50*	*100,39*	*101,54*	*102,70*	*105,05*	*97,88*	*99,81*	*100,93*	*102,06*
kg/m³	*1,1857*	*1,1889*	*1,2463*	*1,3112*	*1,3690*	*1,1789*	*1,1828*	*1,2403*	*1,3052*
m²	*2123,72*	*2123,72*	*2123,72*	*2123,72*	*2123,72*	*6362*	*6362*	*6362*	*6362*
%	*27,7%*	*27,7%*	*27,7%*	*27,7%*	*27,7%*	*38,6%*	*38,6%*	*38,6%*	*38,6%*

Wind speed *25* Temperature *35,16* Pressure *104,34* Air density *1,3623* Blade swept area - $const^{6362}$ Capacity factor - $const^{38,6\%}$ Power output *MWh/year* ***0,000 138,383 1088,695 4132,195 55185,519 0,000 765,446 6059,488 23098,258 228687,888***

Atbasar

Variables Unit Min Low Base High Max Min Low Base High Max

m/s	*0*	*3,48*	*6,89*	*10,69*	*25*	*0*	*3,84*	*7,61*	*11,77*
°C	*-34,755*	*-16,38*	*2,32*	*21,01*	*30,935*	*-35,08*	*-16,7*	*1,99*	*20,68*
kPa	*94,04*	*96,02*	*97,23*	*98,45*	*100,13*	*93,45*	*95,44*	*96,63*	*97,81*
kg/m^3	*1,1471*	*1,1659*	*1,2296*	*1,3027*	*1,3742*	*1,1402*	*1,1597*	*1,2235*	*1,2965*
m^2	*2123,72*	*2123,72*	*2123,72*	*2123,72*	*2123,72*	*6362*	*6362*	*6362*	*6362*
%	*26,6%*	*26,6%*	*26,6%*	*26,6%*	*26,6%*	*37,3%*	*37,3%*	*37,3%*	*37,3%*

Wind speed *25* Temperature *30,61* Pressure *99,42* Air density *1,3674* Blade swept area - $const^{6362}$ Capacity factor - $const^{37,3\%}$ Power output *MWh/year* ***0,000 121,645 995,652 3939,801 53155,499 0,000 681,850 5599,127 21951,549 221866,175***

Zaysan

Variables Unit Min Low Base High Max Min Low Base High Max

m/s	*0*	*2,4*	*5,29*	*8,69*	*25*	*0*	*2,64*	*5,81*	*9,57*
°C	*-31,095*	*-11,18*	*6,56*	*24,31*	*30,965*	*-31,42*	*-11,51*	*6,24*	*23,98*
kPa	*93,80*	*94,69*	*95,81*	*96,93*	*98,59*	*93,27*	*94,14*	*95,23*	*96,31*
kg/m^3	*1,1294*	*1,1352*	*1,1933*	*1,2592*	*1,3501*	*1,1227*	*1,1292*	*1,1874*	*1,2535*
m^2	*2123,72*	*2123,72*	*2123,72*	*2123,72*	*2123,72*	*6362*	*6362*	*6362*	*6362*
%	*16,1%*	*16,1%*	*16,1%*	*16,1%*	*16,1%*	*23,3%*	*23,3%*	*23,3%*	*23,3%*

Wind speed *25* Temperature *30,64* Pressure *97,90* Air density *1,3442* Blade swept area - $const^{6362}$ Capacity factor - $const^{23,3\%}$ Power output *MWh/year* ***0,000 23,548 265,065 1239,920 31652,653 0,000 135,155 1514,904 7146,605 136623,858***

Kyzylorda

Variables Unit Min Low Base High Max Min Low Base High Max

m/s	*0*	*3,68*	*6,97*	*10,45*	*25*	*0*	*4,08*	*7,69*	*11,53*

Wind speed *25* Temperature *°C -22,445 -7,47 10,61 28,68 36,975 -22,77 -7,79 10,28 28,36 36,65*

Pressure *kPa 97,77 98,58 99,73 100,89 103,24 97,22 98,02 99,13 100,25 102,55*

kg/m³	*1,1598*	*1,1645*	*1,2244*	*1,2926*	*1,3586*	*1,1532*	*1,1583*	*1,2184*	*1,2868*
m²	*2123,72*	*2123,72*	*2123,72*	*2123,72*	*2123,72*	*6362*	*6362*	*6362*	*6362*
%	*27,1%*	*27,1%*	*27,1%*	*27,1%*	*27,1%*	*38,4%*	*38,4%*	*38,4%*	*38,4%*

Air density *1,3526* Blade swept

area - $const^{6362}$ Capacity

factor - $const^{38,4\%}$ Power output *MWh/year* ***0,000 146,443 1046,191 3722,348 53568,276 0,000 842,275 5932,381 21118,247 226279,165***

Baikonur

Variables Unit Min Low Base High Max Min Low Base High Max

m/s	*0*	*3,72*	*6,93*	*10,29*	*25*	*0*	*4,08*	*7,65*	*11,33*
°C	*-22,52*	*-8,54*	*9,95*	*28,44*	*35,37*	*-22,84*	*-8,86*	*9,62*	*28,11*
kPa	*98,06*	*98,89*	*100,06*	*101,23*	*103,60*	*97,50*	*98,32*	*99,45*	*100,59*
kg/m³	*1,1698*	*1,1693*	*1,2313*	*1,3019*	*1,3630*	*1,1632*	*1,1632*	*1,2252*	*1,2960*
m²	*2123,72*	*2123,72*	*2123,72*	*2123,72*	*2123,72*	*6362*	*6362*	*6362*	*6362*
%	*26,4%*	*26,4%*	*26,4%*	*26,4%*	*26,4%*	*37,7%*	*37,7%*	*37,7%*	*37,7%*

Wind speed *25* Temperature *35,04* Pressure *102,90* Air density *1,3570* Blade swept

area - $const^{6362}$ Capacity

factor - $const^{37,7\%}$ Power output *MWh/year* ***0,000 147,574 1004,638 3477,617 52210,836 0,000 829,907 5762,240 19800,968 222737,221***

Beyneu

Variables Unit Min Low Base High Max Min Low Base High Max

m/s	*0*	*3,48*	*6,81*	*10,45*	*25*	*0*	*3,84*	*7,53*	*11,53*

°C	*-20,495*	*-5,95*	*11,27*	*28,48*	*37,475*	*-20,82*	*-6,28*	*10,94*	*28,16*
kPa	*98,41*	*99,46*	*100,56*	*101,66*	*103,90*	*97,81*	*98,89*	*99,96*	*101,03*
kg/m³	*1,1652*	*1,1741*	*1,2317*	*1,2967*	*1,3569*	*1,1587*	*1,1681*	*1,2258*	*1,2909*
m²	*2123,72*	*2123,72*	*2123,72*	*2123,72*	*2123,72*	*6362*	*6362*	*6362*	*6362*
%	*26,0%*	*26,0%*	*26,0%*	*26,0%*	*26,0%*	*36,6%*	*36,6%*	*36,6%*	*36,6%*

Wind speed *25* Temperature *37,15* Pressure *103,21* Air density *1,3503* Blade swept area - *const*^{6362} Capacity factor - *const*$^{36,6\%}$ Power output *MWh/year* ***0,000 119,737 941,288 3580,776 51304,531 0,000 674,835 5339,767 20188,664 215270,076***

Shetpe

Variables Unit Min Low Base High Max Min Low Base High Max

m/s	*0*	*3,72*	*7,13*	*10,73*	*25*	*0*	*4,12*	*7,85*	*11,81*
°C	*-18,645*	*-3,59*	*12,13*	*27,86*	*35,375*	*-18,97*	*-3,91*	*11,81*	*27,53*
kPa	*96,93*	*98,27*	*99,23*	*101,19*	*102,18*	*96,34*	*97,70*	*98,63*	*99,57*
kg/m³	*1,1538*	*1,1711*	*1,2118*	*1,2700*	*1,3268*	*1,1473*	*1,1536*	*1,2058*	*1,2641*
m²	*2123,72*	*2123,72*	*2123,72*	*2123,72*	*2123,72*	*6362*	*6362*	*6362*	*6362*

Wind speed *25* Temperature *35,05* Pressure *101,50* Air density *1,3204* Blade swept area - *const*^{6362} Capacity

factor - *const*$^{\%}$ *28,2% 28,2% 28,2% 28,2% 28,2% 39,2% 39,2% 39,2% 39,2% 39,2%*

Power output *MWh/year* ***0,000 158,192 1152,499 4116,848 54397,943 0,000 882,331 6378,965 22773,029 225637,976 Zhanaozen***

Variables Unit Min Low Base High Max Min Low Base High Max

m/s	*0*	*3,6*	*6,89*	*10,41*	*25*	*0*	*4*	*7,61*	*11,45*
°C	*-18,065*	*-4,19*	*12,03*	*28,24*	*36,655*	*-18,39*	*-4,52*	*11,7*	*27,92*
kPa	*96,75*	*97,88*	*98,85*	*99,81*	*101,81*	*96,15*	*97,31*	*98,25*	*99,19*
kg/m³	*1,1448*	*1,1537*	*1,2075*	*1,2678*	*1,3214*	*1,1384*	*1,1477*	*1,2016*	*1,2620*
m²	*2123,72*	*2123,72*	*2123,72*	*2123,72*	*2123,72*	*6362*	*6362*	*6362*	*6362*

%	*26,4%*	*26,4%*	*26,4%*	*26,4%*	*26,4%*	*37,2%*	*37,2%*	*37,2%*	*37,2%*

Wind speed *25* Temperature *36,33* Pressure *101,13* Air density *1,3148* Blade swept area - $const^{6362}$ Capacity factor - $const^{37,2\%}$ Power output *MWh/year* ***0,000 132,259 970,481 3514,232 50730,382 0,000 761,200 5487,682 19630,802 212883,716***

Zhetibay

Variables Unit Min Low Base High Max Min Low Base High Max

m/s	*0*	*3,68*	*7,09*	*10,73*	*25*	*0*	*4,08*	*7,81*	*11,85*
°C	*-16,075*	*-2,35*	*13,26*	*28,87*	*36,095*	*-16,4*	*-2,68*	*12,93*	*28,54*
kPa	*98,51*	*99,69*	*100,71*	*101,73*	*103,85*	*97,92*	*99,11*	*100,11*	*101,10*
kg/m^3	*1,1699*	*1,1734*	*1,2250*	*1,2825*	*1,3350*	*1,1634*	*1,1674*	*1,2191*	*1,2766*
m^2	*2123,72*	*2123,72*	*2123,72*	*2123,72*	*2123,72*	*6362*	*6362*	*6362*	*6362*
%	*28,2%*	*28,2%*	*28,2%*	*28,2%*	*28,2%*	*39,0%*	*39,0%*	*39,0%*	*39,0%*

Wind speed *25* Temperature *35,77* Pressure *103,17* Air density *1,3286* Blade swept area - $const^{6362}$ Capacity factor - $const^{39,0\%}$ Power output *MWh/year* ***0,000 153,403 1145,247 4156,024 54717,334 0,000 860,696 6304,087 23058,581 225342,362***

Eski Ikan

Variables Unit Min Low Base High Max Min Low Base High Max

m/s	*0*	*3,16*	*6,73*	*10,93*	*25*	*0*	*3,48*	*7,41*	*12,05*
°C	*-21,315*	*-2,98*	*12,6*	*28,19*	*35,715*	*-21,64*	*-3,31*	*12,28*	*27,86*
kPa	*94,44*	*95,05*	*96,00*	*96,94*	*98,85*	*93,92*	*94,51*	*95,42*	*96,33*
kg/m^3	*1,1149*	*1,1207*	*1,1704*	*1,2256*	*1,3065*	*1,1085*	*1,1149*	*1,1646*	*1,2202*
m^2	*2123,72*	*2123,72*	*2123,72*	*2123,72*	*2123,72*	*6362*	*6362*	*6362*	*6362*
%	*27,2%*	*27,2%*	*27,2%*	*27,2%*	*27,2%*	*36,8%*	*36,8%*	*36,8%*	*36,8%*

Wind speed *25* Temperature *35,39* Pressure *98,18* Air density *1,3009* Blade swept area - $const^{6362}$ Capacity factor - $const^{36,8\%}$ Power output *MWh/year* ***0,000 89,345 901,353 4043,338 51575,532 0,000 481,943 4860,395 21898,268 208497,513***

Georgievka

Variables Unit Min Low Base High Max Min Low Base High Max

m/s	*0*	*3,04*	*6,17*	*9,69*	*25*	*0*	*3,32*	*6,77*	*10,62*

Wind speed *25* Temperature *°C -34,385 -15,18 2,66 20,49 27,615 -34,71 -15,5 2,33 20,16 27,29*

Pressure *kPa 91,46 92,19 93,13 94,06 95,48 90,94 91,65 92,55 93,45 94,81*

kg/m^3	*1,1060*	*1,1159*	*1,1763*	*1,2450*	*1,3345*	*1,0993*	*1,1099*	*1,1704*	*1,2392*
m^2	*2123,72*	*2123,72*	*2123,72*	*2123,72*	*2123,72*	*6362*	*6362*	*6362*	*6362*
%	*23,2%*	*23,2%*	*23,2%*	*23,2%*	*23,2%*	*32,5%*	*32,5%*	*32,5%*	*32,5%*

Air density *1,3287* Blade swept

area - *const^{6362}* Capacity

factor - *const$^{32,5\%}$* Power output *MWh/year* ***0,000 67,767 597,229 2448,452 45071,796 0,000 368,228 3292,327 13456,324 188211,036***

Ulbi

Variables Unit Min Low Base High Max Min Low Base High Max

m/s	*0*	*1,96*	*4,36*	*7,29*	*23,74*	*0*	*2,16*	*4,84*	*8,01*
°C	*-33,425*	*-17,86*	*-2,17*	*13,53*	*20,365*	*-33,75*	*-18,19*	*-2,49*	*13,21*
kPa	*84,54*	*85,39*	*86,04*	*86,70*	*87,65*	*84,01*	*84,86*	*85,50*	*86,14*
kg/m^3	*1,0403*	*1,0536*	*1,1061*	*1,1652*	*1,2285*	*1,0342*	*1,0479*	*1,1005*	*1,1595*
m^2	*2123,72*	*2123,72*	*2123,72*	*2123,72*	*2123,72*	*6362*	*6362*	*6362*	*6362*
%	*9,7%*	*9,7%*	*9,7%*	*9,7%*	*9,7%*	*14,6%*	*14,6%*	*14,6%*	*14,6%*

Wind speed *25* Temperature *20,04* Pressure *87,04* Air density *1,2225* Blade swept

area - *const^{6362}* Capacity

factor - *const$^{14,6\%}$* Power output *MWh/year* ***0,000 7,176 82,932 408,371 14868,893 0,000 43,009 508,137 2426,784 77788,796***

The wind analysis results revealed potential maximum energy production values at 50 and 100 meters for twenty specified locations. During data analysis and Weibull distribution analysis,

the cumulative distribution function (CDF) was used to determine the *max* value, which was set at 25 m/s. This limitation corresponds to the rated speed (cut-out) at which the selected wind turbines are designed. Moreover, the calculation of air density has an inverse contribution from pressure and temperature values, in which case, for the air density value, the values of the variable are flipped around its base value, as presented in the Table 8.

Table 9. Rank ordered locations by Max Power Output from one Wind turbine MWh/year.

Rank Location ***Max Power output at 50***

m, by V52 – 850kW Location ***Max Power output at <u>100 m, by V90 – 2 MW</u>***

1 *239905,05*

Fort-Shevchenko	*59708,70*	Yereymentau
Yereymentau	*59351,00*	Arkalyk
Arkalyk	*58008,04*	Fort-Shevchenko
Along Caspian sea	*55185,52*	Along Caspian sea
Zhetibay	*54717,33*	Emba
Janatas	*54640,58*	Kyzylorda
Shetpe	*54397,94*	Shetpe
Emba	*54313,30*	Zhetibay

2 *237271,96* 3 *230628,80* 4 *228687,89* 5 *227118,00* 6 *226279,17* 7 *225637,98* 8 *225342,36* 9 Kyzylorda *53568,28* Baikonur-Zhosaly *222737,22*

10 Atbasar *53155,50* Atbasar *221866,17* 11 *220308,22*

Baikonur-Zhosaly	*52210,84*	Janatas
Eski Ikan	*51575,53*	Beyneu
Beyneu	*51304,53*	Zhanaozen
Zhanaozen	*50730,38*	Eski Ikan
Georgievka	*45071,80*	Georgievka

Karkaralinsk	*44667,20*	Karkaralinsk
Zaysan	*31652,65*	Zaysan
Dzungarian Gate	*25703,99*	Dzungarian Gate
Ulbi	*14868,89*	Ulbi

12 *215270,08* 13 *212883,72* 14 *208497,51* 15 *188211,04* 16 *184803,94* 17 *136623,86* 18 *109488,05* 19 *77788,80* 20 Shelek *9358,78* Shelek *55613,64*

Table 9 displays the sorted values by max power output quantity for each location, indicating that Fort-Shevchenko, Yereymentau, Arkalyk, and Along Caspian Sea emerge as the primary leaders in wind energy generation at both 50 and 100 meters. However, Shelek, Ulbi, Dzungarian Gate, Zaysan, Karkaralinsk, and Georgievka sites have the lowest indicators of generating an energy with the same wind turbine types. Regarding the resulted data outcome, it can be stated that Fort-Shevchenko and Yereymentau are considered to be the optimal places to install wind turbines, however, the next section of this research will consider the GHG reduction potential value as another factor and assess the preferences of the DM which is the main part of the Decision Analysis (DA) methodology and its extension theory of Multiattribute Utility (MAUT).

4.3.2. X_2 GHG reduction potential

The examination of the attribute X_2 – GHG Reduction Potential in selected locations represents another crucial step of this study's attribute analysis. This subsection delves into the outcomes derived from the assessment of GHG reduction potential. The analysis of GHG reduction potential will become an important aspect in the context of environmental impact of potential wind farm locations. Results of calculation of this attribute, along with X_1 (potential wind power output), will form the basis for comprehensive decision-making within the Multiattribute Utility Function (MUF) framework. The focus will be on explaining the significance of the GHG reduction potential as another attribute in the selection of optimal locations for wind power generation. The RETScreen Expert software methodology was used to calculate the annual GHG reduction potential, Equation (20).

Table 10. Annual average GHG reduction potential at 50 and 100 meters. ***№ Alternatives***

Average annual GHG emission reduction potential ($tCO_2eq/year$)

	h =
Dzungarian Gate	*120*
Shelek	*143*
Fort-Shevchenko	*238*
Arkalyk	*233*
Yereymentau	*235*
Karkaralinsk	*200*
Janatas	*233*
Emba	*221*
Along Caspian sea	*220*
Atbasar	*222*

Zaysan	*1670,7*
Kyzylorda	*2218,8*
Baikonur	*2187,5*
Beyneu	*2191,8*
Shetpe	*2264,8*
Zhanaozen	*2168,0*
Zhetibay	*2264,3*
Eski Ikan	*2156,0*
Georgievka	*1925,3*

h = 100m

1 *1605,4* 2 *2470,3* 3 *5492,0* 4 *5330,7* 5 *5361,2* 6 *4337,0* 7 *5038,5* 8 *5004,1* 9 *5158,5* 10 *5050,9* 11 *3305,6* 12 *5063,8* 13 *4993,1* 14 *4941,5* 15 *5162,9* 16 *4949,8* 17 *5220,4* 18 *4763,9* 19 *4107,1* 20 Ulbi *1391,7 2313,4*

Nevertheless, due to the limited availability of accessible data, only the average annual GHG emission reduction potential for each location was calculated. In contrast, for the first attribute, the hourly data was employed for each location. The evaluation of the variability of attribute X_2 entailed analyzing average annual data for each location in Kazakhstan spanning from 2019 to 2023. Probability plot approach was used to approximate the distribution of the data and characterize the type of distribution observed at each location in Kazakhstan. Following the construction of the PP plots, it was determined that among the initial twenty locations, seven exhibited adherences to two distinct distribution types: normal and lognormal, respectively. Probability plots (PP) for five year values of GHG emission reduction potential that approximate the distribution type in seven locations are detailed in Appendix K. Locations selected for the further investigation are presented in the map of Kazakhstan Figure 10. To demonstrate the data calculated across the seven locations, Figure 11 presents the potential for GHG emission

reductions in various locations spanning from 2019 to 2023 for wind turbine at 50 meters.

52

Figure 10. Final seven selected locations in the map of Kazakhstan.

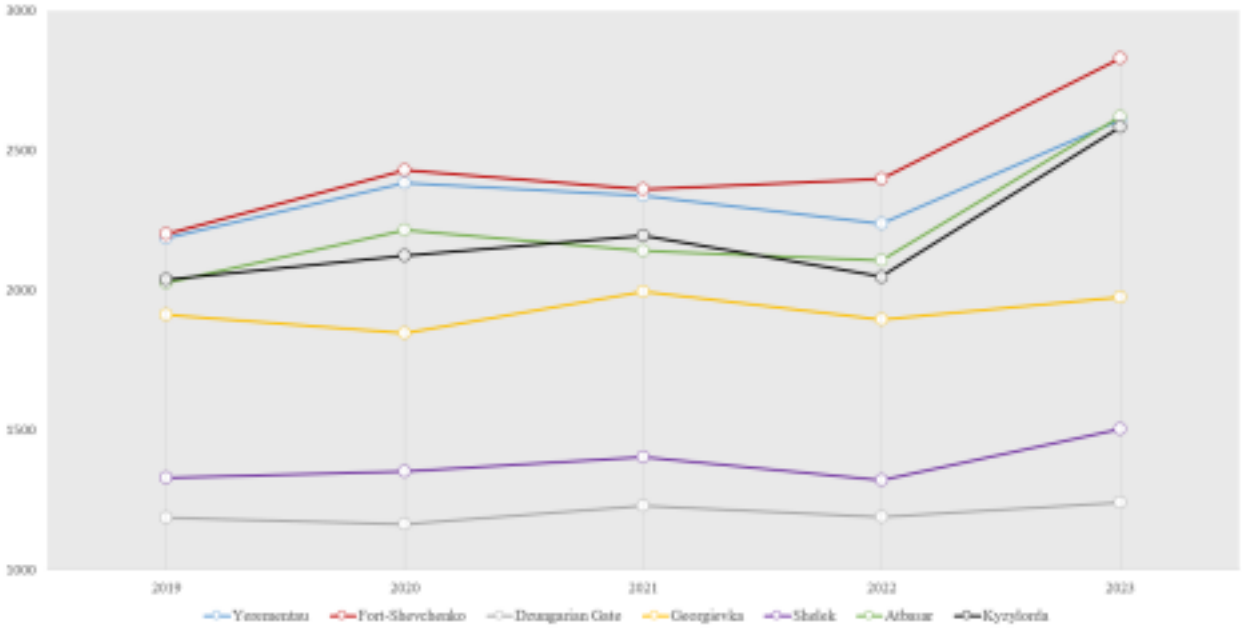

Figure 11. GHG emission reduction potential of wind turbines at 50 meters from 2019 to 2023 for seven locations.

The analysis of Figure 11 reveals that Fort-Shevchenko demonstrates appealing annual GHG emission reduction targets, almost 3000 tCO_2eq/year. This trend is also evident in the potential of Yereymentau. Conversely, Shelek and the Dzungarian Gate demonstrate notably lower indicators

compared to the other locations, not higher than 1500 tCO_2eq/year. While other locations demonstrate figures ranging between 1500 and 2600 tCO_2e/year.

Likewise, with the MAUT methodology employed for the X_1 attribute, employing the method for the X_2 attribute. Which requires the extraction of statistical values, including minimum (min), low, base, high, and maximum (max) from seven selected locations. Table 11 represents a statistical value of GHG emission reduction potential for seven locations.

Table 11. X_2 attribute – GHG reduction potential. Min, low, base, high, and max values average for all alternatives at 50 and 100 meters height.

Dzungarian Gate – Normal Distribution

Variable	*Unit*	*Min*	*Low*	*Base*	*High*	*Max*	*Min*	*Low*	*Base*	*High*	*Max*
GHG reduction potential	*tCO_2eq/year*	*1974,9*	*2249,2*	*2378*							

7134,7

Shelek – Normal Distribution

Variable	*Unit*	*Min*	*Low*	*Base*	*High*	*Max*	*Min*	*Low*	*Base*	*High*	*Max*
GHG reduction potential	*tCO_2eq/year*	*1127*	*1299,3*	*138*							

3739,7

Fort-Shevchenko – Lognormal Distribution

Variable	*Unit*	*Min*	*Low*	*Base*	*High*	*Max*	*Min*	*Low*	*Base*	*High*	*Max*
GHG reduction potential	*tCO_2eq/year*	*1983*	*2249,8*	*2380*							

6937,2

Yereymentau ***– Lognormal Distribution***

Variable	*Unit*	*Min*	*Low*	*Base*	*High*	*Max*	*Min*	*Low*	*Base*	*High*	*Max*
GHG reduction potential	*tCO_2eq/year*	*1781*	*2164,2*	*2352*							

7013,4

Atbasar – Lognormal Distribution

Variable	*Unit*	*Min*	*Low*	*Base*	*High*	*Max*	*Min*	*Low*	*Base*	*High*	*Max*
GHG reduction potential	*tCO_2eq/year*	*1512*	*1974*	*2213*							

6505,8

Kyzylorda – Lognormal Distribution

Variable Unit Min Low Base High Max Min Low Base High Max

GHG reduction

potential $tCO_2eq/year$ *1511 1958,8 2190,1 2448,7 3175,2 3034 4319,8 5026,9 5849,7 8326* ***Georgievka – Lognormal Distribution***

Variable Unit Min Low Base High Max Min Low Base High Max GHG reduction

potential $tCO_2eq/year$ *1709,2 1857,1 1924,5 1994,3 2166,9 3536,4 3924,9 4104,6 4292,5 4764*

The average GHG emission reduction potential calculated for 50 and 100 meter wind turbines for the 2019–2023 timeframe are shown in Table 12.

Table 12. Average GHG emission reduction potential by one wind turbine for seven locations, $tCO_2eq/year$.

№ Location Average GHG emission	***reduction potential, $tCO_2eq/year$ at 50 meters***	***Location Average GHG***	***emission reduction potential, $tCO_2eq/year$ at 100 meters***
1 *5583,8*			
Fort-Shevchenko	*2445*	Fort-Shevchenko	
Dzungarian Gate	*1202,6*	Dzungarian Gate	
Yereymentau	*2352,3*	Yereymentau	
Atbasar	*2222,4*	Kyzylorda	
Kyzylorda	*2198,8*	Atbasar	
Georgievka	*1925,3*	Georgievka	

2 *1605,4* 3 *5361,2* 4 *5063,8* 5 *4948,4* 6 *4107,1* 7 Shelek *1382,6* Shelek *2313,3*

4.4. Decision tree construction

The construction of a decision tree (DT) is one of the steps in the decision-making process,

the visual representation of the criteria and decision pathways involved in selecting optimal locations for wind power plant installations. This process outlines the systematic approach taken to develop the decision tree, focusing on the primary attributes, wind power output (X_1), and GHG reduction potential (X_2). Firstly, decision tree starts with the identification of decision nodes, representing critical points where choices are made. These nodes serve as key junctures where the decision

making process unfolds. The attribute's values high, base, and, low calculated for the Pout in Table 6 will be location in the X_1 nodes. Similarly, with the X_2 values of GHG emission reduction potential in Table 11. The first part of the decision tree is alternatives (i.e. potential locations for

WPP), in this case seven locations are considered. Next from each alternative are nodes connecting to attribute X_1 with high (0.25), base (0.5) and low (0.25) probability values, indicating a 25% probability for high and low classes, and 50% chance for the base class. These probabilities guide the model's classification decisions as it moves data through the tree. Finally, nodes from each probability value of attribute X_1 are connected to attribute X_2. Figure 12 represent a simplified decision tree for seven alternatives.

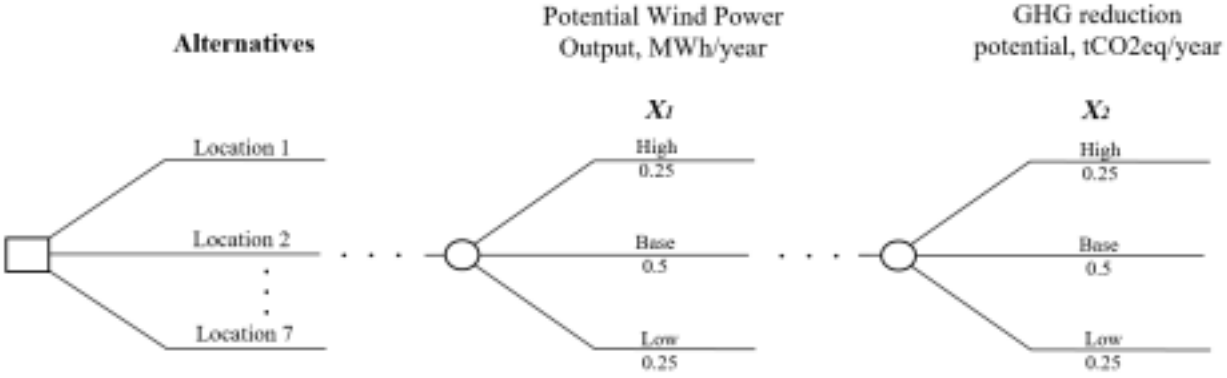

Figure 12. Simplified decision tree for seven alternatives (locations).

4.5. Multiattribute utility function construction

In the multiattribute utility theory (MAUT) methodology, the Decision Maker (DM) plays a major role in providing valuable insights through the completion of the decision analysis process by answering a questionnaire. The interview protocol was approved by the Nazarbayev University Institutional Review Board for Ethical Conduct (IREC), and subsequently, an

interview with an expert in the energy field (decision maker) was carried out at Nazarbayev University. There will be three questionnaires for the decision maker (DM). First, utility independence questionnaire for the DM is presented in Appendix E, this questionnaire serves to determine the decision maker's preference for whether attributes are utility independent on each other. Four cases of utility independencies (UI) was described by Abdildin and Abbas 2013 [81]. Mutual utility independence, partial utility independence two cases: one-switch UI and boundary UI, and complete utility dependence. Two scenarios and a question are presented to the decision maker, and by examining the DM's responses, utility interdependence of the two attributes is determined.

An interview with the expert was conducted and the results of the first questionnaire on utility independence were reviewed. DM responses on the questionnaire: Scenario 1 – Project B, Scenario 2 – Project B, Final question – No. After examination of the results, the expert's preferences resulted complete mutual UI among the attributes X_1 and X_2, which corresponds to a multilinear form of a multiattribute utility function, in Equation (22). For the two attribute case this equation will have the following form:

$$u(x_1, x_2) = k_1 u_1(x_1) + k_2 u_2(x_2) + k_1 k_2 u_1(x_1) u_2(x_2) \quad (23)$$

where every attribute, is UI of its complement, and $u_{ii}(x_{ii}) = u(x_{ii} | \bar{x}_{ii})$, and the scaling constants will be equal to $k_1 = u(x_1^*, x_2^0)$, $k_2 = u(x_1^0, x_2^*)$, and $k_{12} = 1 - k_1 - k_2$.

A next elicitation questionnaire is used to find the utility function $u_{iiii}(x_{ii})$ for each attribute, which are specified in Appendix F for attribute X_1, and Appendix G for attribute X_2 respectively. After conducting an interview with the expert, the following values were identified $x_{0.25}$, $x_{0.5}$, and $x_{0.75}$, these values will serve as points in the plot and will form the complete function for single

attribute. Table 12 represents a response of DM on elicitation questionnaire. Values of $x^*$and x^0 are the maximum of maximum and minimum of minimum values of each attribute that was calculated in Table 8 and Table 11.

Table 13. X_1 and X_2 attributes DM's responses (bold) to elicitation questionnaire, $x_{ii.iiii}$,

$\boldsymbol{\square\square_{\square\square.\square\square}}$ *and* $\boldsymbol{\square\square_{\square\square.\square\square\square\square}}$.

Quartiles	Values at 50 meters $\square\square_1$ MWh/year $\square\square_2$ tCO_2eq/year	Values at 100 meters $\square\square_1$ MWh/year $\square\square_2$ tCO_2eq/year
$\square\square^*$	*59 708 3 239,26*	*239 905 8 326*
$\square\square_{\square\square.\square\square\square\square}$	***45 000 2 700***	***180 000 6 600***
$\square\square_{\square\square.\square\square}$	***30 000 2 200***	***120 000 4 900***
$\square\square_{\square\square.\square\square\square\square}$	***15 000 1 650***	***60 000 3 150***
$\square\square^0$	*0 1 127,27*	*0 1411,93*

After receiving the responses from decision maker (DM), as highlighted in bold in Table 13, the process of constructing a single attribute utility function can be initiated through curve fitting approximation, as depicted in Figures 13 to 16. The derived functions reveal a consistent

linear form across all attributes, indicating the decision makers' risk-neutral behavior during responses to the elicitation questionnaire. This characteristic is evident in both the graphical representations (Figures 13 to 16) and in Table 13.

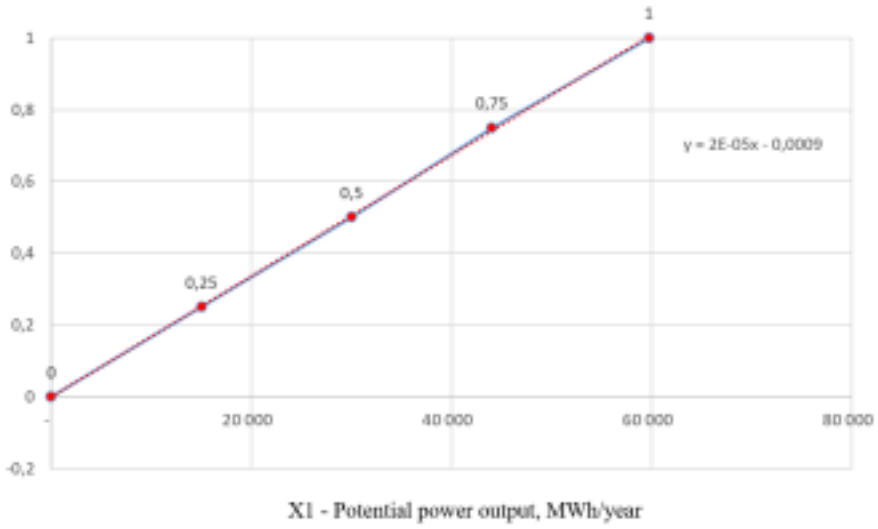

Figure 13. Curve fitting for X_1 attribute at 50 meters.

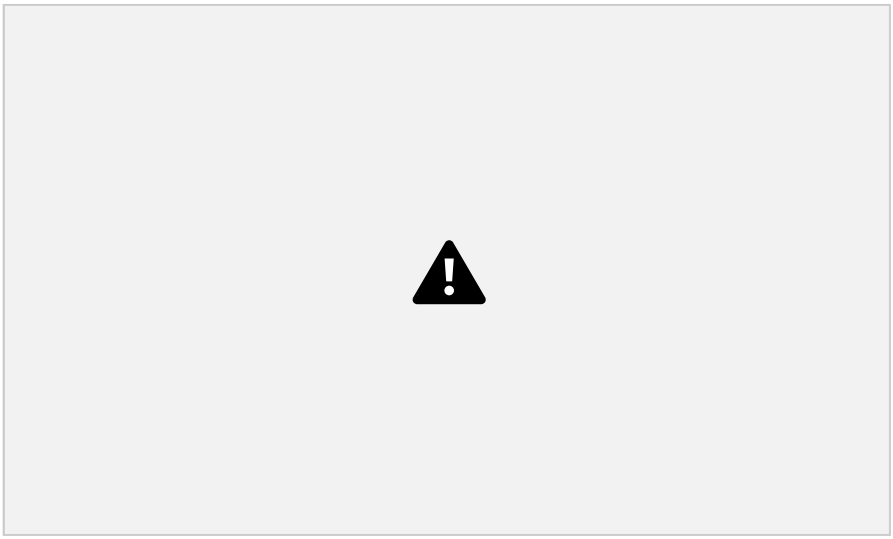

Figure 14. Curve fitting for X_1 attribute at 100 meters.

Based on the resulted DM preferences from curve fittings for X_1 attribute (Figure 13 – 14) the expected single attribute utility can be calculated, by using decision tree from Figure 11 and high, base, and low values from Table 8 for X_1 attribute. The approximated functions based on the

preferences of the DM the expected utility for each location on 50 and 100 meters can be calculated. Expected utility function is calculated using formula below:

$$\text{EU}(X_{\text{location}}) = 0.25 * u_{\text{low}}(x_{\text{low}}) + 0.5 * u_{\text{base}}(x_{\text{base}}) + 0.25 * u_{\text{high}}(x_{\text{high}}) \quad (24)$$

where the x_{ij} value is *high*, *base*, and *low* values of an attribute, in case of X_1 – values of potential power output (P_{location}) of each location from Table 8, and in case of X_2 – values of annual average GHG reduction potential (Δ_{location}) from Table 11, and the probabilities in the decision tree Figure 11.

After evaluating the responses gathered from the elicitation questionnaire, it was observed that the decision-maker (DM) provided linear responses, meaning that to attributes X_1 and X_2 DM is risk-neutral position. For instance, from Figure 13, WPP at 50 meters the utility function is expressed as:

$$u_{x1}(x_1) = x_1 * x_1 - x_1 \quad (25)$$

where $\diamond\diamond_1 = 0{,}00002$, and $\diamond\diamond_1 = 0{,}0009$, and the $\diamond\diamond_1$value is high, base, and low values of potential power output ($\diamond\diamond_{\diamond\diamond\diamond\diamond\diamond\diamond}$) of each location.

Similar with the WPP at 100 meters the function from Figure 14:

$$\diamond\diamond_{\diamond\diamond 1}(\diamond\diamond_1) = \diamond\diamond_1 * \diamond\diamond_1 - \diamond\diamond_1 \quad (26)$$

where $\diamond\diamond_1 = 0{,}000004$, and $\diamond\diamond_1 = 0{,}00008$. Extracted utility functions can be applied into Equation (24), in order to calculate the expected single attribute utility. Table 14 represents an expected utility function values for 50 and 100 meters' wind power plants.

Table 14. Single-attribute expected utility values at 20 locations for 50 and 100 meters for X_1 attribute.

№ Location	***X_1 Expected Utility at 50 meters***	***X_1Expected Utility at 100 meters***
1	*0,00*	
Dzungarian Gate	*0,00*	
Shelek	*0,00*	
Fort-Shevchenko	*0,04*	
Arkalyk	*0,04*	
Yereymentau	*0,04*	
Karkaralinsk	*0,02*	
2	*0,00*	
3	*0,05*	
4	*0,04*	
5	*0,04*	
6	*0,02*	
7 Janatas	*0,03*	*0,04*

8 Emba	*0,03*	*0,03*
9	*0,04*	
Along Caspian sea	*0,03*	
Atbasar	*0,03*	
Zaysan	*0,01*	
Kyzylorda	*0,03*	
Baikonur	*0,03*	
Beyneu	*0,03*	

Shetpe	*0,03*
Zhanaozen	*0,03*
Zhetibay	*0,03*
Eski Ikan	*0,03*
Georgievka	*0,02*

10 *0,03* 11 *0,01* 12 *0,03* 13 *0,03* 14 *0,03* 15 *0,04* 16 *0,03* 17 *0,04* 18 *0,03* 19 *0,02* 20 Ulbi *0,00 0,00*

The following utility function was determined for the second X_2 attribute GHG reduction potential at 50 meters from Figure 15:

$$\text{[illegible]}_{\text{[illegible]}2}(\text{[illegible]}_2) = \text{[illegible]}_2 * \text{[illegible]}_2 - \text{[illegible]}_2 \quad (27)$$

where $\text{[illegible]}_2 = 0{,}0005$, and $\text{[illegible]}_2 = 0{,}5349$.

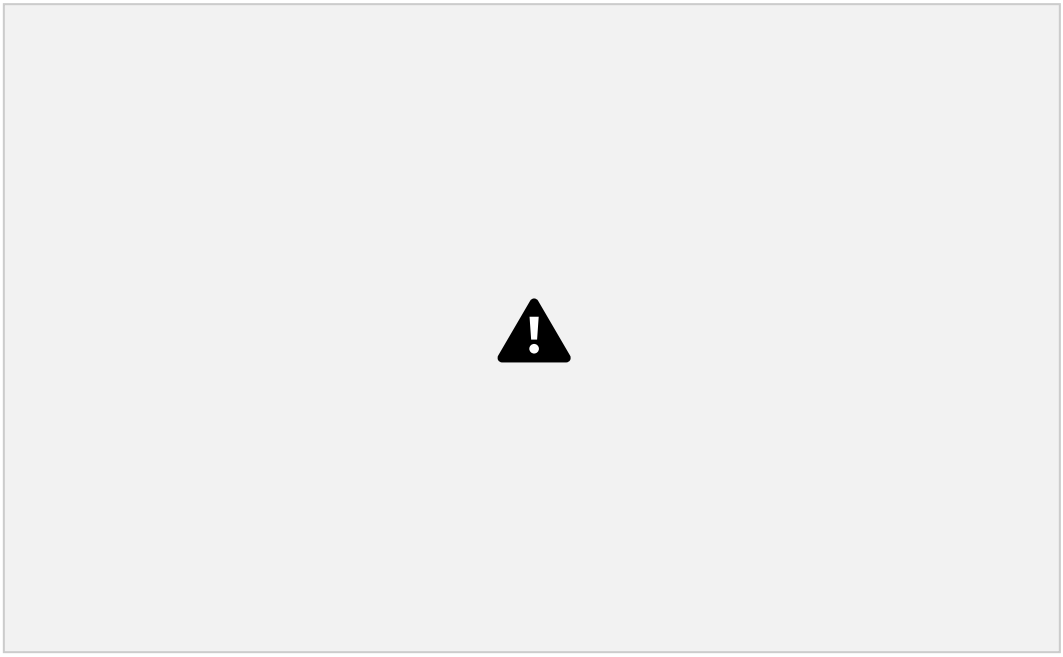

Figure 15. Curve fitting for X_2 attribute at 50 meters.

Similarly, with the X_2 attribute GHG reduction potential for 100 meters from Figure 16:

$$\text{EU}_{X_2}(X_2) = X_2 * X_2 - X_2 \quad (28)$$

where $X_2 = 0{,}0001$, and $X_2 = 0{,}2057$. Table 15 represents the expected single-attribute utility values for X_2 attribute. Expected utility values were calculated for seven locations due to a lack of data on GHG emissions at the locations, which was discussed in subsection 4.3.2 X_2 GHG emission reduction potential.

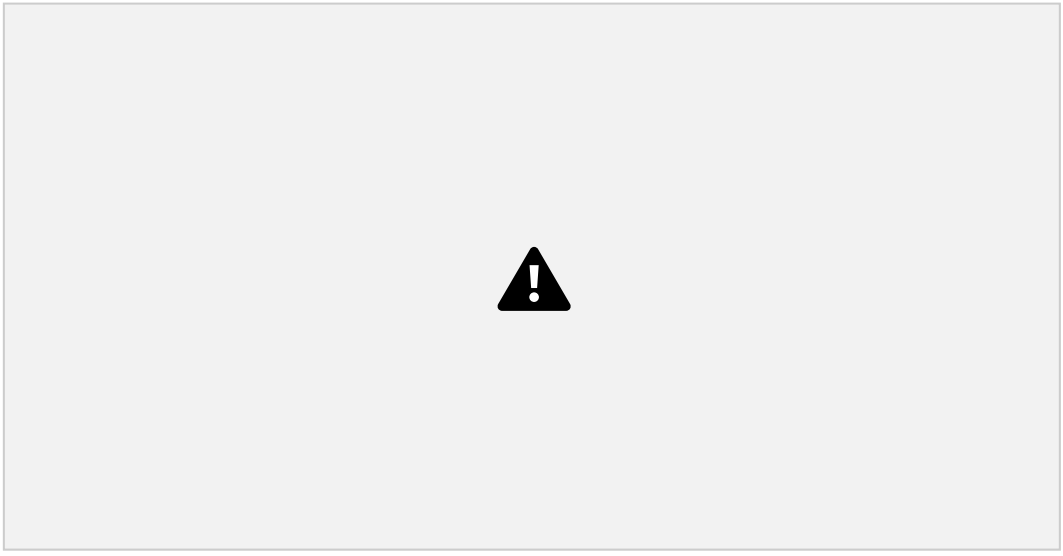

Figure 16. Curve fitting for X_2 attribute at 100 meters.

Table 15 Single-attribute expected utility at seven locations for 50 and 100 meters for X_2 attribute.

№ Location X_2 Expected Utility at 50 meters Location X_2 Expected Utility at 100 meters

1 *0,3435*

Fort-Shevchenko	*0,6554*	Fort-Shevchenko
Dzungarian Gate	*0,6552*	Dzungarian Gate
Yereymentau	*0,6413*	Yereymentau
Atbasar	*0,5754*	Kyzylorda
Kyzylorda	*0,5636*	Atbasar
Georgievka	*0,4277*	Georgievka

2 *0,3433* 3 *0,3304* 4 *0,2999* 5 *0,2889* 6 *0,2050* 7 Shelek *0,1562* Shelek *0,0253*

Recall the derived multilinear form, Equation (23) $$$$ = $$$$($$$$*, $$$$0), and $$$$ = 1 − $$$$ − $$$$, from which the constant scaling coefficients were assessed from the DM. The coefficient

assessment questionnaire is demonstrated in detail in Appendix H. The question: *what probability (p) makes you indifferent between: (1) receiving* ($$$$1*, $$$$20) *surely for a wind turbine at 50 meters and (2) lottery between* ($$$$1*, $$$$2*) with p and* ($$$$10, $$$$20) *with (1 - p)?*

The DM response was $$ = 95%, so the $$$$1 = $$($$$$1*, $$$$20) = 0.95, and same with $$$$2, with $$$$2 = $$($$$$10, $$$$2*) = 0.01 where $$ = 1%. In this questionnaire the DM's responses were same to the WPP projects at 50 and 100 meters' height.

Finally, all the elements are available to construct multiattribute utility function that will determine the optimal location for installing the WPP in Kazakhstan. Using an Equation (23) the utility functions and scaling constants for the WPP at 50 meters' height can be displayed in the following expression.

$$$$($$$$1, $$$$2) = $$$$1$$$$1($$$$1) + $$$$2$$$$2($$$$2) +

$$$$1$$$$2$$$$1($$$$1)$$$$2($$$$2) (29) where $$$$1($$$$1) = $$1 ∗ $$$$1 − $$$$1;

where $$$$1 = 0,00002, and $$$$1 = 0,0009;

$$$$2($$$$2) = $$2 ∗ $$$$2 − $$$$2;

where $$$$2 = 0,0005, and $$$$2 = 0,5349;

$$$$1 = $$($$$$1*, $$$$20) = 0.95; $$$$2 = $$($$$$10, $$$$2*) = 0.1; $$$$1$$$$2 = 0.04.

The MUF for WPP calculated for 100 meters' height:

$$$$($$$$1, $$$$2) = $$$$1$$$$1($$$$1) + $$$$1$$$$2($$$$2) +

$$$$1$$$$2$$$$1($$$$1)$$$$2($$$$2) (30) where $$$$1($$$$1) = $$1 ∗ $$$$1 − $$$$1;

where $$$$1 = 0,000004, and $$$$1 = 0,00008;

$$\text{ }_{2}(\text{ }_{2}) = \text{ }_{2} * \text{ }_{2} - \text{ }_{2};$$

where $\text{ }_{2} = 0{,}0001$, and $\text{ }_{2} = 0{,}2057$;

$$\text{ }_{1} = \text{ }(\text{ }_{1}^{*}, \text{ }_{2}^{0}) = 0.95; \text{ }_{2} = \text{ }(\text{ }_{1}^{0}, \text{ }_{2}^{*}) = 0.1; \text{ }_{1}\text{ }_{2} = 0.04.$$

62

4.6. Multiattribute utility function expected utility

The calculation of the Expected Utility E(U) for two attributes is a final step in quantifying the overall utility of potential WPP sites, and identifying an optimal decision among all alternatives. With obtained the true preferences of the Decision Maker (DM) and the single attribute utility functions developed for two attributes the final MUF can be calculated. The expected utility calculation creates the contributions of both attributes, providing overall measure of a particular wind farm location. The subsequent comparison of Expected Utilities across different sites will guide the final decision-making process, leading to the identification of optimal locations for WPP installations for 50 and 100 meters' height wind turbine types. The expected multiattribute utility values calculated using Equations (29) and (30) for seven locations are presented in Table 16.

Table 16. Expected utility at seven locations for 50 and 100 meters.

№ Location	***Expected utility of WPP at 50 m Location***	***Expected utility of WPP at 100 m***
1	*0,0484*	Fort-Shevchenko
Fort-Shevchenko	*0,0498*	Fort-Shevchenko
Yereymentau	*0,0451*	Yereymentau
Atbasar	*0,0343*	Kyzylorda
Kyzylorda	*0,0337*	Atbasar
Georgievka	*0,0213*	Georgievka
Dzungarian Gate	*0,0080*	Dzungarian Gate

2 *0,0458* 3 *0,0355* 4 *0,0353* 5 *0,0192* 6 *0,0059* 7 Shelek *0,0043* Shelek *0,0044*

Figure 17 demonstrates the comparison of expected utility values for seven locations WPP at 50 and 100 meters' height. According to the histogram illustrating the expected multiattribute utility values, it is evident that the optimal location for the setting up of wind turbines in Kazakhstan is the Fort-Shevchenko wind power project, 0.0498 for 50 meters, and 0.0484 for 100 meters respectfully. This based on the factors, including the considerable potential for reducing greenhouse gas emissions and the potential power output. It is noteworthy that Fort-Shevchenko is unique not only for its favorable attributes, but also for its geographical location located on the shore of the Caspian Sea, which helps ensure efficient distribution of wind potential. Following Yeremenetau site takes the second place, which exhibits slightly lower potential compared to Fort-

Shevchenko. It is important to mention that the expected utility for a wind farm in the Yereymentau location is greater if the wind turbine is installed at a height of 100 meters.

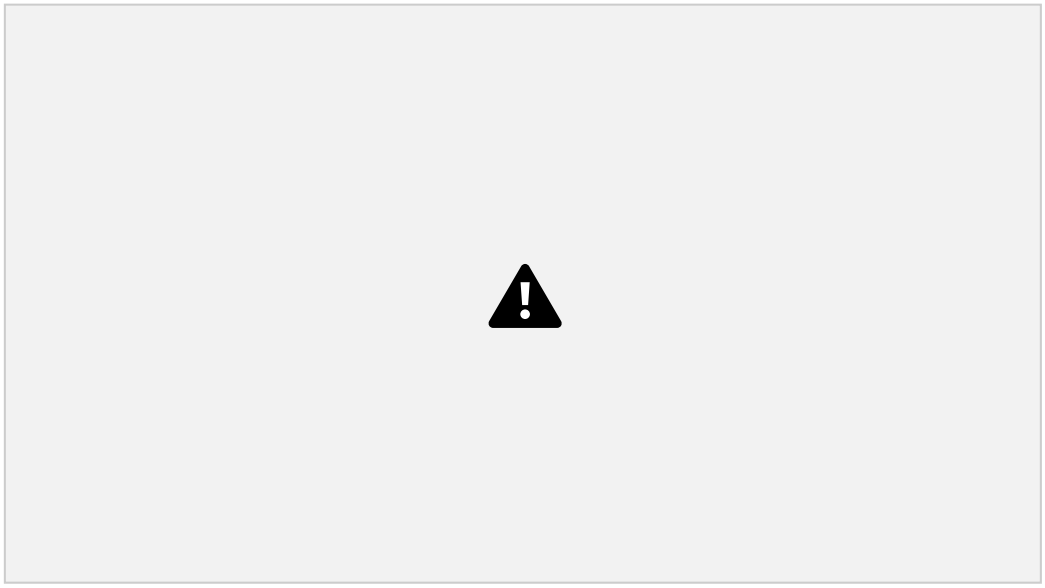

Figure 17. Comparison of expected multiattribute utility values across seven locations for WPP at 50 and 100 m height.

Atbasar and Kyzylorda share the third position, with only a marginal difference of 0.56% observed between them (0.0355 versus 0.0353 for WPP at 100 meters). This slight change

emphasizes how crucial it is to choose locations to maximize the overall efficacy of wind power projects.

In contrast, Georgievka demonstrates low expected utility that is half that of Fort Shevchenko, with expected utility at 100 meters' hub height of 0.0192. Lastly, the Dzungarian Gate and Shelek sites present significantly lower expected multi-attribute utility values among all seven locations assessed. Even though these locations might not have as many advantages as others, but its contribution in the analysis offers valuable comparison data regarding the diverse wind power potential of Kazakhstan.

In conclusion, the research highlights the diversity of Kazakhstan's wind energy potential. As a result, Fort-Shevchenko becomes the optimal location, followed by Yeremenetau and other locations. This study provides an answer to the research question of using MAUT decision analysis methodology to select optimal locations and provides valuable information for making informed decisions to stimulate wind energy projects and reduce GHG emissions across the entire energy sector in Kazakhstan.

Chapter 5 – Discussion

The study comprehensively reveals the main goal of this research problem, which answers the question of formulating a mathematical model based on the multiattribute utility of the theory (MAUT). The purpose of constructed model is to determine the optimal sites for the location of wind power plants (WPPs) in Kazakhstan. The patterns and distribution of these changes in wind speed and the potential for reducing greenhouse gas emissions in Kazakhstan were also studied. As a result of this research, the optimal locations for installing wind farms in Kazakhstan were identified. Moreover, this study examined both the potential for clean wind power generation in Kazakhstan over a five-year period and the reduction of GHG emissions, which has been widely discussed over the past decades. Unlike past studies, the selection of optimal locations was based on a decision analysis approach, specifically application of decision analysis extension – multiattribute utility theory (MAUT). The theory extracts utility from each alternative (i.e. location) and also incorporates the application of the DMs actual preferences into the mathematical model. The results showed that the Fort-Shevchenko location in Kazakhstan is the most optimal for installing a wind power plant. The data obtained indicate that, based on the

preferences of the DM, who is normally an expert in the field of research, this location is the best location. The choice of this location by the constructed model is due to the fact that this area has an excellent wind patterns, and its geographical location on the shores of the Caspian Sea.

Notably, the expected utility of different locations responds differently to each wind turbine height. For instance, the model prefers a wind turbine at a height of 50 meters for Fort-Shevchenko over a turbine at a height of 100 meters (0.0498 vs. 0.0484). Conversely, for Yereymentau the expected utility for a wind turbine at the height of 100 meters is higher than for a wind turbine at 50 meters. This means that although the electricity production is higher for a 100-meter wind turbine, it may not always give the expected result for the DM. Regarding the regions of Kazakhstan, mainly the northern regions and the eastern border adjacent to the Caspian Sea are promising areas for the installation of wind power plants in terms of potential power generation and power factor. The study also observed a correlation indicating that wind speeds in numerous studied locations in 2023 were notably higher compared to the preceding years from 2019. A notable observation is the observed seasonal variability in wind patterns across Kazakhstan: weaker winds in the summer months and increased wind activity in the autumn and winter seasons.

A similar pattern can be seen in the potential to minimize GHG emissions in 2023, there is a rise in this potential. These results provide valuable material on the geographic distribution of wind energy resources in Kazakhstan.

Moreover, the results suggest that the southern region of Kazakhstan, specifically Dzungarian Gate and Shelek, exhibit lower suitability for wind power installations in terms of expected utility. However, based on the results of similar studies [31], [34], these locations were recommended for the installation of wind farms, contrasting with the present results. Nevertheless previous study have shown promising energy production potential in the Fort-Shevchenko and Yereymentau areas [49], which support the results obtained in the current study.

Nonetheless, the study had some limitations. Initially, 20 locations were selected for analysis to determine their suitability for wind turbine installations. However, due to limited data on the greenhouse gas (GHG) reduction potential for each location, only the seven locations were included in the final calculations. In addition, the distribution of these locations was

approximated using a probability plotting. Despite existing limitations in the current study, several recommendations can be made to expand future research in this area. First, efforts should be made to improve data collection methods to provide a more complete set of data for analysis, such as the use of data capture systems on each location. Additionally, possible collaboration with relevant stakeholders to collect more detailed information on the potential for greenhouse gas emissions reductions in a wider range of locations. Furthermore, it is recommended to explore alternative methodologies for assessing greenhouse gas emission reduction potential, such as remote sensing techniques.

In conclusion, this study aims to achieve its main goal of formulating a mathematical model based on MAUT to determine the optimal locations for installing wind power plants (WPPs) in Kazakhstan. By studying the patterns and distribution of wind speed and potential to reduce GHG emissions, the study identified the optimal locations for wind farms. Unlike previous studies, this study used a decision analysis approach, specifically applying an extension of decision analysis, MAUT, which incorporates true decision makers' preferences into the model. The results show that Fort-Shevchenko is the most optimal location for installing wind power plants due to its favorable wind conditions and geographical location on the Caspian Sea shore.

However, despite the significance of the results, the study challenged limitations of lack of data availability, which resulted in seven sites being included in the analysis. Recommendations for future research include improving data collection methods, collaborating with stakeholders to collect detailed information, and exploring alternative methodologies for assessing GHG reduction potential. These efforts will help improve the accuracy and completeness of future research in this area, which will ultimately contribute to the sustainable development of wind energy in Kazakhstan.

Chapter 6 – Conclusions

The main goal of this research was to identify optimal locations for installing wind power plants in Kazakhstan using a decision analysis. The study comprehensively explored Kazakhstan's wind energy capacity and the potential of reducing a greenhouse gas emission. Moreover, the decision-making methodology of Multi-attribute utility theory (MAUT) was

applied to identify the expected utility values of each location based on the main attributes, and integration of decision maker's (DM) true preferences through questionnaires to determine the most suitable location, with Fort-Shevchenko identified as the most optimal for a 50-meter height among seven explored locations. This research has significant relevance in considering the challenges of sustainable energy production and GHG emission mitigation. By applying the decision analysis for identification of optimal WPP locations, it may contribute to the Kazakhstan's efforts on the way to effectively integrate renewable energy sources and reduce the level of GHG emissions, which will make Kazakhstan's energy sector relevant to the SDGs.

Future research could focus on improving decision analysis methodology and alternative methodology for calculating GHG emission reduction potential. Possibly also including additional attributes for the MUF function, such as economic feasibility. There is also the possibility of developing a web application for decision analysis for choosing the type of wind turbines and choosing a location for installation based on personal preferences. Many investors from Kazakhstan, together with officials, experts in the energy sector, and environmentalists, may find this study beneficial. The findings can be used by policymakers and private investors to formulate initiatives aimed at integration of RES, and business experts can use the results of this study to make optimal decisions with wind power investments.

The comprehensive analysis conducted in this study highlights the significance of using relevant decision analysis methodologies such as MAUT to make optimal decisions in renewable energy development sector. By prioritizing sustainability and efficiency, the optimal location can accelerate the transition to a green and sustainable energy, benefiting both current and future generations.

References

[1] P. A. Owusu and S. Asumadu-Sarkodie, "A review of renewable energy sources, sustainability issues and climate change mitigation," *Cogent Eng.*, vol. 3, no. 1, p. 1167990, Dec. 2016, doi: 10.1080/23311916.2016.1167990.

[2] IEA (2022), "For the first time in decades, the number of people without access to electricity is set to increase in 2022," IEA. [Online]. Available:

https://www.iea.org/commentaries/for-the-first-time-in-decades-the-number-of-people without-access-to-electricity-is-set-to-increase-in-2022
[3] United Nations, Department of Economic and Social Affairs, Population Division (2022)., "World Population Prospects 2022 Summary of Results," no. UN DESA/POP/2022/TR/NO. 3., 2022, [Online]. Available: https://www.un.org/development/desa/pd/sites/www.un.org.development.desa.pd/files/wpp 2022_summary_of_results.pdf
[4] IEA (2023), "Electricity Market Report 2023," IEA, Paris, License: CC BY 4.0, Feb. 2023. [Online]. Available: https://www.iea.org/reports/electricity-market-report-2023 [5] IEA (2021), "Electricity production – Electricity Information: Overview," License: CC BY 4.0, 2021. [Online]. Available: https://www.iea.org/reports/electricity-information overview/electricity-production
[6] L. Al-Ghussain, "Global warming: review on driving forces and mitigation: Global Warming: Review on Driving Forces and Mitigation," *Environ. Prog. Sustain. Energy*, vol. 38, no. 1, pp. 13–21, Jan. 2019, doi: 10.1002/ep.13041.
[7] World Meteorological Organization (WMO), *State of the Global Climate 2022*. Geneva, Switzerland: WMO, 2023. [Online]. Available: https://library.wmo.int/idurl/4/66214 [8] *WMO statement on the state of the global climate in 2021 State of the Global Climate 2021*. Geneva, Switzerland: World Meteorological Organization (WMO), 2022. [9] B. Trewin *et al.*, "Headline Indicators for Global Climate Monitoring," *Bull. Am. Meteorol. Soc.*, vol. 102, no. 1, pp. E20–E37, Jan. 2021, doi: 10.1175/BAMS-D-19-0196.1. [10] IEA (2023), "CO2 Emissions in 2022," Paris, License: CC BY 4.0. [Online]. Available: https://www.iea.org/reports/co2-emissions-in-2022
[11] A. Rossati, "Global Warming and Its Health Impact," *Int. J. Occup. Environ. Med.*, vol. 8, no. 1, pp. 7–20, Jan. 2017, doi: 10.15171/ijoem.2017.963.
[12] P. Wallemacq and R. House, "Economic Losses, Poverty & Disasters (1998–2017)," *United Nations Office for Disaster Risk Reduction (UNISDR) and Centre for Research on the Epidemiology of Disasters (CRED).*, 2018.
[13] H. Ritchie, P. Rosado, and M. Roser, "Emissions by sector," *Our World Data*, Sep. 2023, [Online]. Available: https://ourworldindata.org/emissions-by-sector
[14] UN General Assembly (2015)., "Transforming our world: The 2030 agenda for sustainable development," UN General Assembly, 2015. [Online]. Available: https://documents-dds ny.un.org/doc/UNDOC/GEN/N15/291/89/PDF/N1529189.pdf?OpenElement
[15] R. Haas, G. Resch, C. Panzer, S. Busch, M. Ragwitz, and A. Held, "Efficiency and effectiveness of promotion systems for electricity generation from renewable energy sources – Lessons from EU countries," *Energy*, vol. 36, no. 4, pp. 2186–2193, Apr. 2011, doi: 10.1016/j.energy.2010.06.028.
[16] E. Papadis and G. Tsatsaronis, "Challenges in the decarbonization of the energy sector," *Energy*, vol. 205, p. 118025, Aug. 2020, doi: 10.1016/j.energy.2020.118025.

[17] N. L. Panwar, S. C. Kaushik, and S. Kothari, "Role of renewable energy sources in environmental protection: A review," *Renew. Sustain. Energy Rev.*, vol. 15, no. 3, pp. 1513–1524, Apr. 2011, doi: 10.1016/j.rser.2010.11.037.
[18] E. Dogan, T. Luni, M. T. Majeed, and P. Tzeremes, "The nexus between global carbon and renewable energy sources: A step towards sustainability," *J. Clean. Prod.*, vol. 416, p.

137927, Sep. 2023, doi: 10.1016/j.jclepro.2023.137927.
[19] IRENA (2023), “Renewable energy statistics 2023, International Renewable Energy Agency,” Abu Dhabi, ISBN: 978-92-9260-537-7 ISBN: 978-92-9260-537-7. [Online]. Available: https://mc-cd8320d4-36a1-40ac-83cc-3389-cdn-endpoint.azureedge.net/-/media/Files/IRENA/Agency/Publication/2023/Jul/IRENA_Renewable_energy_statistics_2 023.pdf?rev=7b2f44c294b84cad9a27fc24949d2134
[20] Paris Agreement to the United Nations Framework Convention on Climate Change, in 16, no. 16–1104. 2015.
[21] Z. Kabir, N. Sultana, and I. Khan, “Chapter 3 - Environmental, social, and economic impacts of renewable energy sources,” in *Renewable Energy and Sustainability*, I. Khan, Ed., Elsevier, 2022, pp. 57–85. doi: 10.1016/B978-0-323-88668-0.00009-7.
[22] IEA (2023), “Global CO2 emissions rose less than initially feared in 2022 as clean energy growth offset much of the impact of greater coal and oil use,” Paris, License: CC BY 4.0. [Online]. Available: https://www.iea.org/news/global-co2-emissions-rose-less-than initially-feared-in-2022-as-clean-energy-growth-offset-much-of-the-impact-of-greater-coal and-oil-use
[23] M. El Haj Assad, M. Alhuyi Nazari, and M. A. Rosen, “Chapter 1 - Applications of renewable energy sources,” in *Design and Performance Optimization of Renewable Energy Systems*, M. E. H. Assad and M. A. Rosen, Eds., Academic Press, 2021, pp. 1–15. doi: 10.1016/B978-0-12-821602-6.00001-8.
[24] A. Sahin, “Progress and recent trends in wind energy,” *Prog. Energy Combust. Sci.*, vol. 30, no. 5, pp. 501–543, 2004, doi: 10.1016/j.pecs.2004.04.001.
[25] T. M. Letcher, “Chapter 1 - Why wind energy,” in *Wind Energy Engineering (Second Edition)*, T. M. Letcher, Ed., Academic Press, 2023, pp. 3–10. doi: 10.1016/B978-0-323-99353-1.00025-6.
[26] H.-Y. Chan, S. B. Riffat, and J. Zhu, “Review of passive solar heating and cooling technologies,” *Renew. Sustain. Energy Rev.*, vol. 14, no. 2, pp. 781–789, Feb. 2010, doi: 10.1016/j.rser.2009.10.030.
[27] A. Evans, V. Strezov, and T. J. Evans, “Assessment of sustainability indicators for renewable energy technologies,” *Renew. Sustain. Energy Rev.*, vol. 13, no. 5, pp. 1082–1088, Jun. 2009, doi: 10.1016/j.rser.2008.03.008.
[28] M. Cengiz and M. Mamis, “Price-Efficiency Relationship for Photovoltaic Systems on a Global Basis,” *Int. J. Photoenergy*, vol. 2015, pp. 1–12, Nov. 2015, doi: 10.1155/2015/256101.
[29] J. N. Rogers *et al.*, “An assessment of the potential products and economic and environmental impacts resulting from a billion ton bioeconomy,” *Biofuels Bioprod. Biorefining*, vol. 11, no. 1, pp. 110–128, Jan. 2017, doi: 10.1002/bbb.1728.
[30] M. Laldjebaev, R. Isaev, and A. Saukhimov, “Renewable energy in Central Asia: An overview of potentials, deployment, outlook, and barriers,” *Energy Rep.*, vol. 7, pp. 3125–3136, Nov. 2021, doi: 10.1016/j.egyr.2021.05.014.

[31] X. Jianzhong, A. Assenova, and V. Erokhin, “Renewable Energy and Sustainable Development in a Resource-Abundant Country: Challenges of Wind Power Generation in

Kazakhstan," *Sustainability*, vol. 10, no. 9, p. 3315, Sep. 2018, doi: 10.3390/su10093315.
[32] B. Satuyeva, C. Sauranbayev, I. A. Ukaegbu, and H. S. V. S. K. Nunna, "Energy 4.0: Towards IoT Applications in Kazakhstan," *Procedia Comput. Sci.*, vol. 151, pp. 909–915, Jan. 2019, doi: 10.1016/j.procs.2019.04.126.
[33] R. I. Mukhamediev, R. Mustakayev, K. Yakunin, S. Kiseleva, and V. Gopejenko, "Multi Criteria Spatial Decision Making Supportsystem for Renewable Energy Development in Kazakhstan," *IEEE Access*, vol. 7, pp. 122275–122288, 2019, doi: 10.1109/ACCESS.2019.2937627.
[34] M. Karatayev and M. L. Clarke, "A review of current energy systems and green energy potential in Kazakhstan," *Renew. Sustain. Energy Rev.*, vol. 55, pp. 491–504, Mar. 2016, doi: 10.1016/j.rser.2015.10.078.
[35] "World Bank Climate Change Knowledge Portal." Accessed: Nov. 03, 2023. [Online]. Available: https://climateknowledgeportal.worldbank.org/
[36] H. Ritchie, M. Roser, and P. Rosado, "CO_2 and Greenhouse Gas Emissions," 2020. [Online]. Available: https://ourworldindata.org/co2-and-other-greenhouse-gas-emissions [37] Y. G. Abdildin, S. A. Nurkenov, and A. Kerimray, "ANALYSIS OF GREEN TECHNOLOGY DEVELOPMENT IN KAZAKHSTAN," *Int. J. Energy Econ. Policy*, vol. 11, no. 3, pp. 269–279, Apr. 2021, doi: 10.32479/ijeep.10897.
[38] "The share of renewable energy in Kazakhstan will reach 6 by 2025%," gov.egov.kz. Accessed: Nov. 04, 2023. [Online]. Available: https://betaegov.kz/memleket/entities/energo/news/details/dolya-vie-v-kazahstane-k-2025-godu-dostignet-6
[39] Global Wind Atlas (2023), "Mean Wind Speed." [Online]. Available: https://globalwindatlas.info/en/area/Kazakhstan
[40] T. Burton, D. Sharpe, N. Jenkins, and E. Bossanyi, *Wind energy: handbook*. Chichester New York: J. Wiley, 2001. [Online]. Available: https://library.uniteddiversity.coop/Energy/Wind/Wind_Energy_Handbook.pdf [41] N. Kurmanov, U. Aliyev, A. Satbayeva, G. Kabdullina, and D. Baxultanov, "ENERGY INTENSITY OF KAZAKHSTAN'S GDP: FACTORS FOR ITS DECREASE IN A RESOURCE-EXPORT DEVELOPING ECONOMY," *Int. J. Energy Econ. Policy*, vol. 10, no. 5, pp. 447–453, Aug. 2020, doi: 10.32479/ijeep.9817.
[42] A. Akhmetov, Y. Uchiyama, and K. Okajima, "Wind Power Development in Kazakhstan: Potential and Obstacles," Jul. 2011.
[43] 231, "Energy Resource Guide - Kazakhstan - Renewable Energy." Accessed: Nov. 20, 2023. [Online]. Available: https://www.trade.gov/energy-resource-guide-kazakhstan renewable-energy
[44] "Renewable energy sources to account for 15% of Kazakhstan energy balance by 2030 — Alikhan Smailov - Official Information Source of the Prime Minister of the Republic of Kazakhstan." Accessed: Nov. 20, 2023. [Online]. Available: https://primeminister.kz/en/news/renewable-energy-sources-to-account-for-15-of kazakhstan-energy-balance-by-2030-alikhan-smailov-24599
[45] T. K. Boomsma, N. Meade, and S.-E. Fleten, "Renewable energy investments under different support schemes: A real options approach," *Eur. J. Oper. Res.*, vol. 220, no. 1, pp. 225–237, Jul. 2012, doi: 10.1016/j.ejor.2012.01.017.

[46] “Development of renewable energy sources,” gov.egov.kz. Accessed: Nov. 20, 2023. [Online]. Available: https://betaegov.kz/memleket/entities/energo/activities/4910 [47] “Financial Settlement Center of Renewable Energy LLP.” Accessed: Nov. 20, 2023. [Online]. Available: https://rfc.kz/en/vie/prices/fixed-rates
[48] J. Cochran, “Kazakhstan’s Potential for Wind and Concentrated Solar Power”. [49] H. H. Pourasl and V. M. Khojastehnezhad, “Techno-economic analysis of wind energy potential in Kazakhstan,” *Proc. Inst. Mech. Eng. Part J. Power Energy*, vol. 235, no. 6, pp. 1563–1576, Sep. 2021, doi: 10.1177/09576509211001598.
[50] D. Turgali, A. Kopeyeva, D. Dikhanbayeva, and L. Rojas-Solórzano, “Potential impact of global warming on wind power production in Central Asia,” *Environ. Prog. Sustain. Energy*, vol. 40, no. 4, p. e13626, 2021, doi: 10.1002/ep.13626.
[51] A. E. Abbas, “Constructing Multiattribute Utility Functions for Decision Analysis,” in *Risk and Optimization in an Uncertain World*, J. J. Hasenbein, P. Gray, and H. J. Greenberg, Eds., INFORMS, 2010, pp. 62–98. doi: 10.1287/educ.1100.0070.
[52] H. Ronald A, “IN PRAISE OF THE OLD TIME RELIGION,” in *Utility Theories: Measurements and Applications*, Kluwer, Boston, 1992, pp. 27–55.
[53] Y. A. Kaplan, “Calculation of Weibull distribution parameters at low wind speed and performance analysis,” *Proc. Inst. Civ. Eng. - Energy*, vol. 175, no. 4, pp. 195–204, Nov. 2022, doi: 10.1680/jener.21.00010.
[54] D. Mohammed, A. S. M. Abdelaziz, E. Mohammed, and E. Elmostapha, “Analysis of wind speed data and wind energy potential using Weibull distribution in Zagora, Morocco,” *Int. J. Renew. Energy Dev.*, vol. 8, no. 3, pp. 267–273, Oct. 2019, doi: 10.14710/ijred.8.3.267-273.
[55] M. La-ongkaew, S.-A. Niwitpong, and S. Niwitpong, “Confidence intervals for the difference between the coefficients of variation of Weibull distributions for analyzing wind speed dispersion,” *PeerJ*, vol. 9, p. e11676, Jul. 2021, doi: 10.7717/peerj.11676.
[56] M. Gökçek, A. Bayülken, and Ş. Bekdemir, “Investigation of wind characteristics and wind energy potential in Kirklareli, Turkey,” *Renew. Energy*, vol. 32, no. 10, pp. 1739–1752, Aug. 2007, doi: 10.1016/j.renene.2006.11.017.
[57] A. Ucar and F. Balo, “Evaluation of wind energy potential and electricity generation at six locations in Turkey,” *Appl. Energy*, vol. 86, no. 10, pp. 1864–1872, Oct. 2009, doi: 10.1016/j.apenergy.2008.12.016.
[58] W. Wang and T. Okaze, “Statistical analysis of low-occurrence strong wind speeds at the pedestrian level around a simplified building based on the Weibull distribution,” *Build. Environ.*, vol. 209, p. 108644, Feb. 2022, doi: 10.1016/j.buildenv.2021.108644.
[59] M. H. Soulouknga, S. O. Oyedepo, S. Y. Doka, and T. C. Kofane, “Assessment of Wind Energy Potential in the Sudanese Zone in Chad,” *Energy Power Eng.*, vol. 09, no. 07, pp. 386–402, 2017, doi: 10.4236/epe.2017.97026.
[60] S. A. Akdağ and A. Dinler, “A new method to estimate Weibull parameters for wind energy applications,” *Energy Convers. Manag.*, vol. 50, no. 7, pp. 1761–1766, Jul. 2009, doi: 10.1016/j.enconman.2009.03.020.
[61] A. Aziz, D. Tsuanyo, J. Nsouandele, I. Mamate, R. Mouangue, and P. Elé Abiama, “Influence of Weibull parameters on the estimation of wind energy potential,” *Sustain.*

Energy Res., vol. 10, no. 1, p. 5, Mar. 2023, doi: 10.1186/s40807-023-00075-y.
[62] Y. Li, X. Huang, K. F. Tee, Q. Li, and X.-P. Wu, "Comparative study of onshore and offshore wind characteristics and wind energy potentials: A case study for southeast coastal

region of China," *Sustain. Energy Technol. Assess.*, vol. 39, p. 100711, Jun. 2020, doi: 10.1016/j.seta.2020.100711.
[63] K. Mohammadi, O. Alavi, A. Mostafaeipour, N. Goudarzi, and M. Jalilvand, "Assessing different parameters estimation methods of Weibull distribution to compute wind power density," *Energy Convers. Manag.*, vol. 108, pp. 322–335, Jan. 2016, doi: 10.1016/j.enconman.2015.11.015.
[64] Minister of Natural Resources Canada, *Clean Energy Project Analysis RETScreen® Engineering & Cases Textbook Third Edition*. Minister of Natural Resources Canada 2001 - 2005., 2005. [Online]. Available: https://publications.gc.ca/collections/collection_2007/nrcan-rncan/M154-13-2005E.pdf
[65] W. Tong, Ed., *Wind power generation and wind turbine design*. Southhampton: Wit Press, 2010.
[66] D. P. Zafirakis, "Energy Yield of Contemporary Wind Turbines," in *Comprehensive Renewable Energy*, Elsevier, 2022, pp. 124–171. doi: 10.1016/B978-0-12-819727-1.00152-7.
[67] M. E. Okorie, F. Inambao, and Z. Chiguvare, "Evaluation of Wind Shear Coefficients, Surface Roughness and Energy Yields over Inland Locations in Namibia," *Procedia Manuf.*, vol. 7, pp. 630–638, 2017, doi: 10.1016/j.promfg.2016.12.094.
[68] S. L. Garrett, "Ideal Gas Laws," in *Understanding Acoustics: An Experimentalist's View of Sound and Vibration*, S. L. Garrett, Ed., in Graduate Texts in Physics. , Cham: Springer International Publishing, 2020, pp. 333–356. doi: 10.1007/978-3-030-44787-8_7.
[69] R. B. Stull, *Practical meteorology: an algebra-based survey of atmospheric science*. Vancouver: UBC, 2017.
[70] T. A. Guinn, D. J. Halperin, and C. G. Herbster, "Climatology of Estimated Altimeter Error due to Nonstandard Temperatures," *J. Appl. Meteorol. Climatol.*, vol. 60, no. 3, pp. 377–390, Mar. 2021, doi: 10.1175/JAMC-D-20-0159.1.
[71] G. Lente and K. Ősz, "Barometric formulas: various derivations and comparisons to environmentally relevant observations," *ChemTexts*, vol. 6, no. 2, p. 13, Jun. 2020, doi: 10.1007/s40828-020-0111-6.
[72] W. Christian, *Hand-book on statistical distributions for experimentalists*. Particle Physics Group Fysikum University of Stockholm., 1996. [Online]. Available: https://www.stat.rice.edu/~dobelman/textfiles/DistributionsHandbook.pdf [73] M. L. Parry, Intergovernmental Panel on Climate Change, World Meteorological Organization, and United Nations Environment Programme, Eds., *Climate change 2007: impacts, adaptation and vulnerability: summary for policymakers, a report of Working Group II of the Intergovernmental Panel on Climate Change and technical summary, a report accepted by Working Group II of the IPCC but not yet approved in detail: part of the Working Group II contribution to the fourth assessment report of the Intergovernmental Panel on Climate Change*. S.l.: WMO : UNEP, 2007.
[74] G. Rediske, H. P. Burin, P. D. Rigo, C. B. Rosa, L. Michels, and J. C. M. Siluk, "Wind

power plant site selection: A systematic review," *Renew. Sustain. Energy Rev.*, vol. 148, p. 111293, Sep. 2021, doi: 10.1016/j.rser.2021.111293.
[75] "Appendix II: IEC Classification of Wind Turbines," in *Wind Resource Assessment and Micro-Siting*, John Wiley & Sons, Ltd, 2015, pp. 269–270. doi: 10.1002/9781118900116.app2.

[76] J. L. Cohon, "Multi-Attribute Utility Theory and Multi-Criteria Decision Making," in *Theory and Practice in Policy Analysis: Including Applications in Science and Technology*, M. G. Morgan, Ed., Cambridge: Cambridge University Press, 2017, pp. 155–184. doi: 10.1017/9781316882665.007.
[77] A. E. Abbas, "The Multiattribute Utility Tree," *Decis. Anal.*, vol. 8, no. 3, pp. 180–205, Sep. 2011, doi: 10.1287/deca.1110.0211.
[78] J. von Neumann and O. Morgenstern, *Theory of Games and Economic Behavior: 60th Anniversary Commemorative Edition*, Princeton University Press, Princeton. 1947. [79] Y. G. Abdildin and A. E. Abbas, "Analysis of decision alternatives of the deep borehole filter restoration problem," *Energy*, vol. 114, pp. 1306–1321, Nov. 2016, doi: 10.1016/j.energy.2016.08.034.
[80] R. L. Keeney and H. Raiffa, *Decisions with multiple objectives: preferences and value tradeoffs*. Cambridge [England] ; New York, NY, USA: Cambridge University Press, 1993. [81] Y. G. Abdildin and A. E. Abbas, "Canonical Multiattribute Utility Functions: Enumeration, Verification, and Application," *Procedia Comput. Sci.*, vol. 18, pp. 2288–2297, 2013, doi: 10.1016/j.procs.2013.05.400.
[82] A. E. Abbas, "General decompositions of multiattribute utility functions with partial utility independence," *J. Multi-Criteria Decis. Anal.*, vol. 17, no. 1–2, pp. 37–59, 2010, doi: 10.1002/mcda.452.
[83] Global Wind Atlas (2023), "GIS files & API access." [Online]. Available: https://globalwindatlas.info/en/download/gis-files
[84] "Kazakhstan Cities Database | Simplemaps.com." Accessed: Nov. 08, 2023. [Online]. Available: https://simplemaps.com/data/kz-cities
[85] "Download data by country | DIVA-GIS." Accessed: Nov. 08, 2023. [Online]. Available: https://www.diva-gis.org/gdata
[86] "NASA POWER | Docs | Methodology | Data Sources - NASA POWER | Docs." Accessed: Feb. 10, 2024. [Online]. Available: https://power.larc.nasa.gov/docs/methodology/data/sources/
[87] "POWER | DAVe." Accessed: Feb. 10, 2024. [Online]. Available: https://power.larc.nasa.gov/beta/data-access-viewer/
[88] "MERRA-2." Accessed: Feb. 10, 2024. [Online]. Available: https://gmao.gsfc.nasa.gov/reanalysis/MERRA-2/
[89] L. Bauer, "Vestas V90 - 2,00 MW - Wind turbine." Accessed: Feb. 10, 2024. [Online]. Available: https://en.wind-turbine-models.com/turbines/16-vestas-v90
[90] L. Bauer, "Vestas V52 - 850,00 kW - Wind turbine." Accessed: Feb. 10, 2024. [Online]. Available: https://en.wind-turbine-models.com/turbines/71-vestas-v52
[91] S. Filom, S. Radfar, R. Panahi, E. Amini, and M. Neshat, "Exploring Wind Energy

Potential as a Driver of Sustainable Development in the Southern Coasts of Iran: The Importance of Wind Speed Statistical Distribution Model," *Sustainability*, vol. 13, no. 14, p. 7702, Jul. 2021, doi: 10.3390/su13147702.

Appendices

Appendix A. Map of Kazakhstan, with road (thin black line), railroad (red line), and wind speed at 50 meters, using QGIS 3.32.3. Sources: [83], [84], [85], [86], [87], [88]

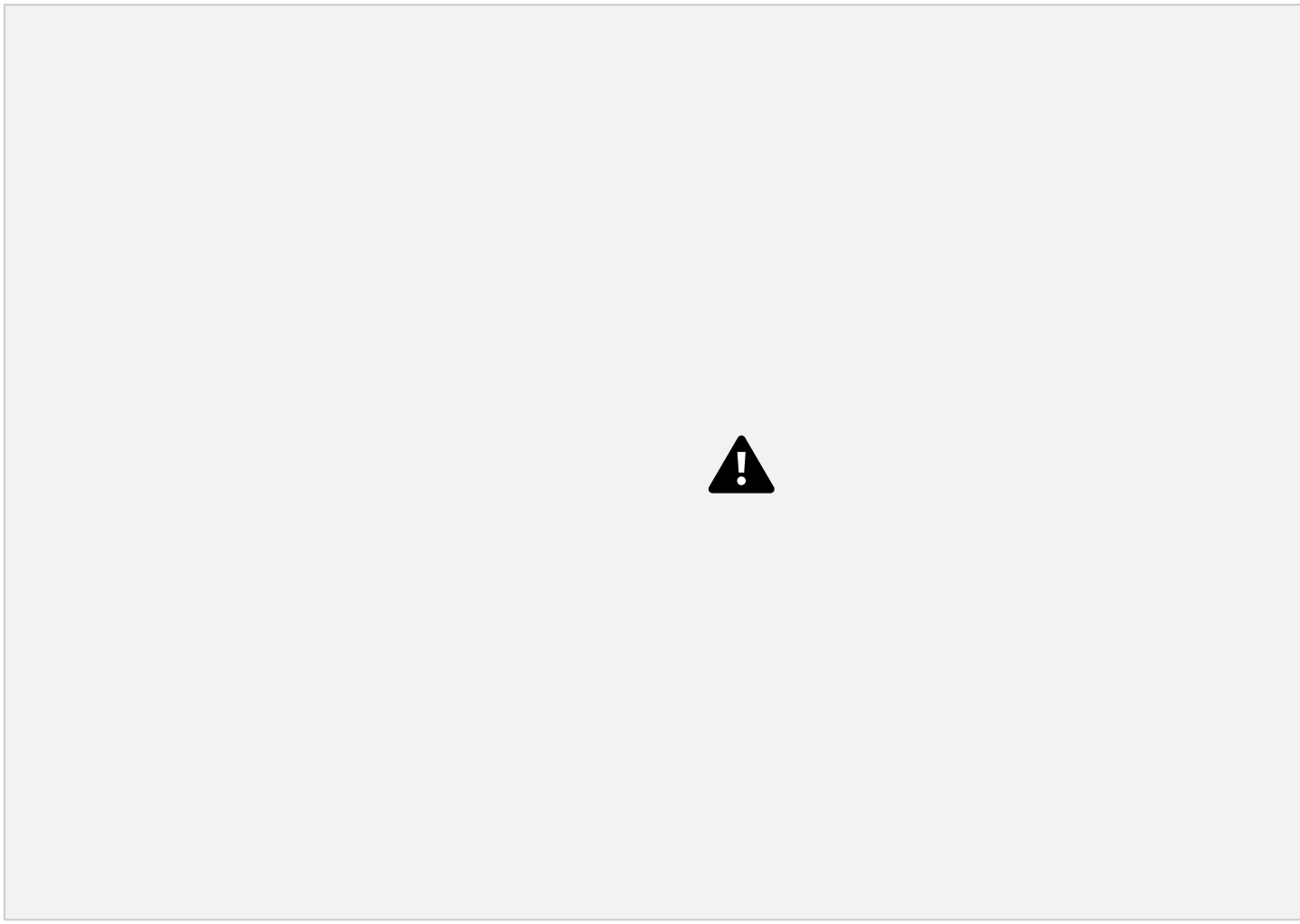

Appendix B. Map of Kazakhstan, with road (thin black line), railroad (red

line), and wind speed at 50 meters (> 7 m/s), using QGIS 3.32.3. Sources: [83], [84], [85], [86], [87], [88]

76

Appendix C. Map of Kazakhstan, with road (thin black line), railroad (red line), and wind speed at 100 meters, using QGIS 3.32.3. Sources: [83], [84], [85], [86], [87], [88]

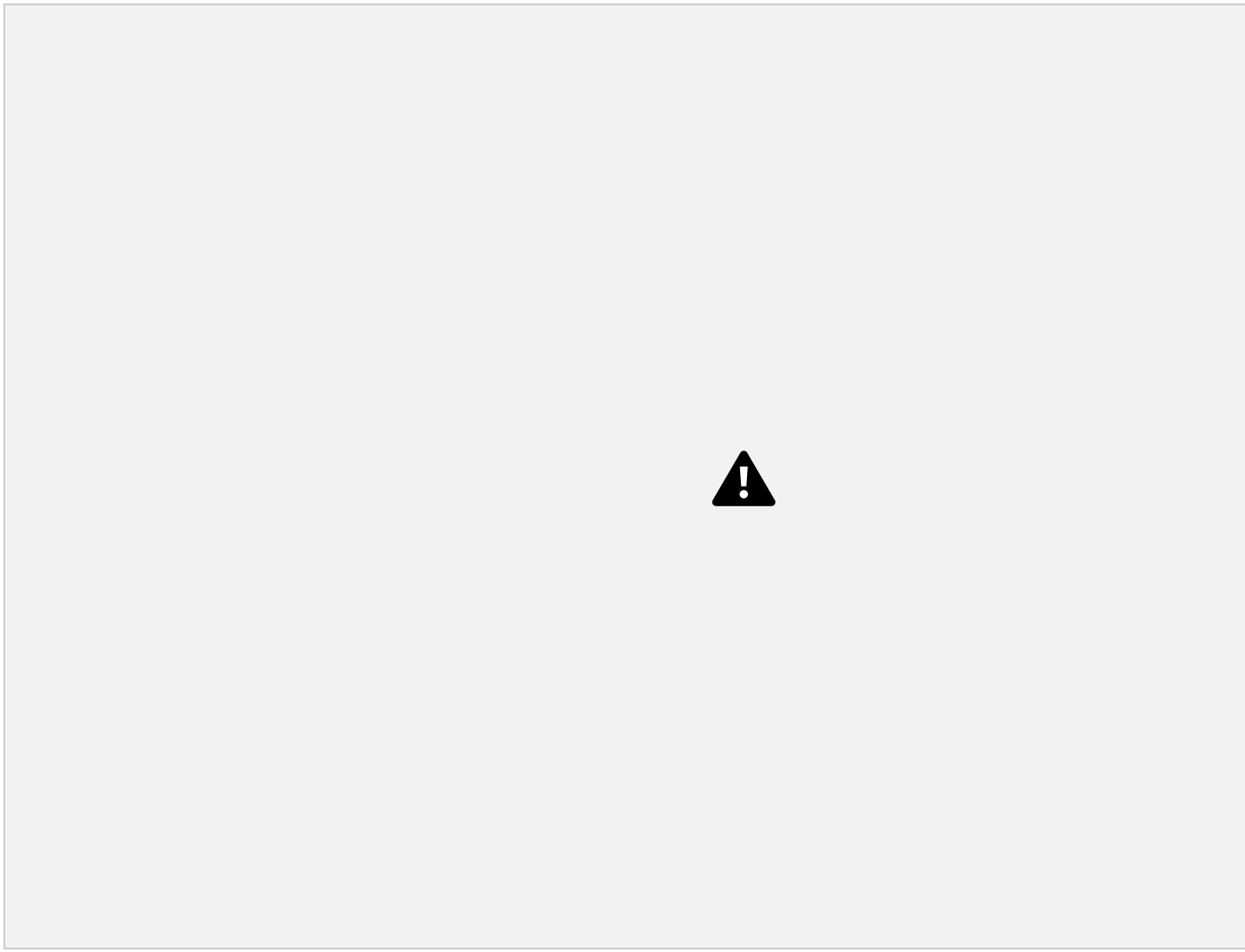

77

Appendix D. Map of Kazakhstan, with road (thin black line), railroad (red line), and wind speed at 100 meters (> 7 m/s), using QGIS 3.32.3. Sources: [83], [84], [85], [86], [87], [88]

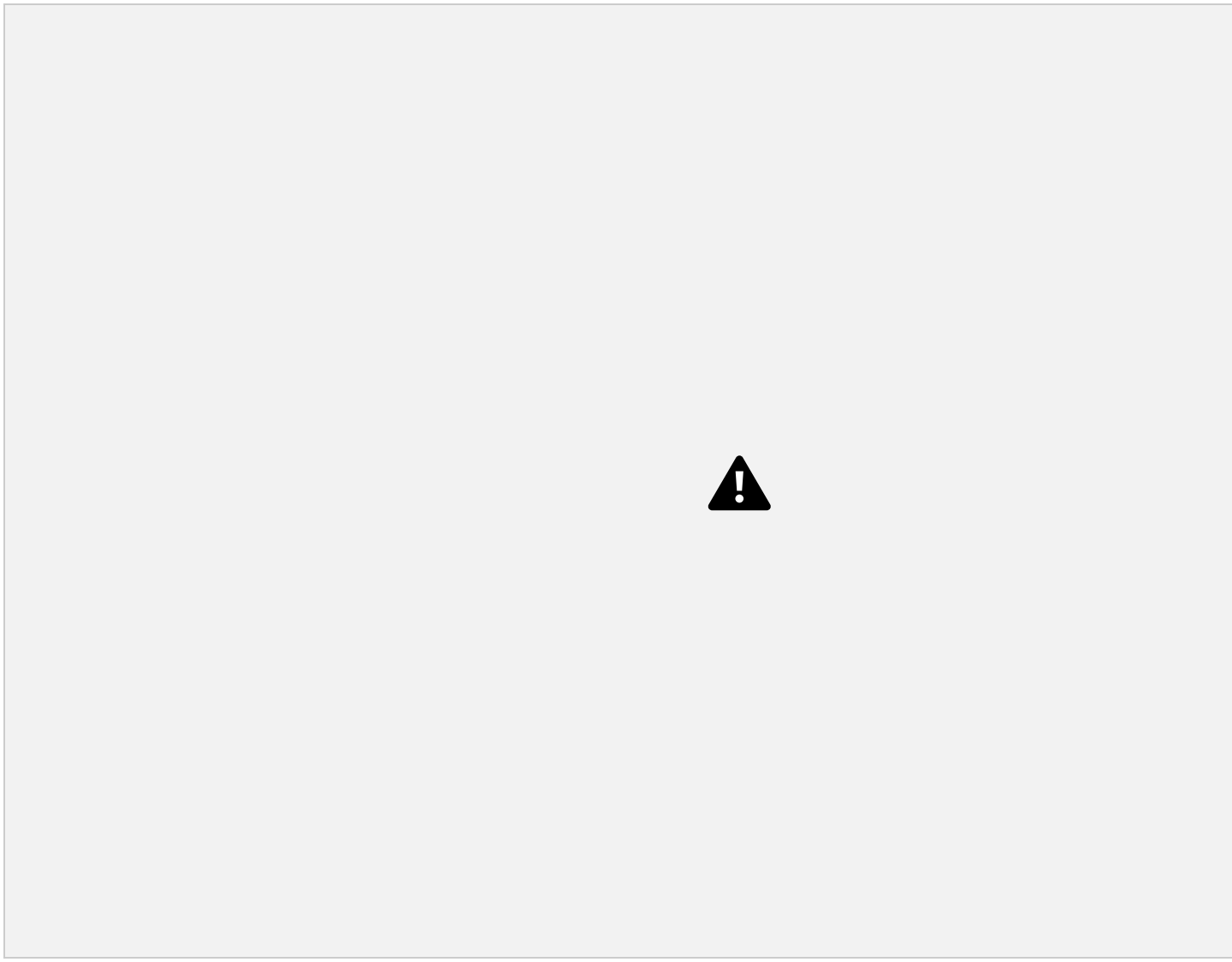

78

Appendix E. Utility independence questionnaire for 50 meters. Source: Adapted from [79]

The purpose of this questionnaire lies on determining a dependence/interdependence between the attributes. There are two main attributes that will be included in the research of selecting optimal locations for the installation of wind power plants (WPP). Attribute X_1 pertains to the potential power output of a wind turbine, measured in megawatt-hours per year (MWh/year), and attribute X_2 signifies the avoided greenhouse gas (GHG) emissions resulting from the operation of the wind turbine, measured in tons of carbon dioxide equivalent per year (tCO2eq/year). These values were calculated for one wind turbine installed at height of 50 meters.

Attribute values will be presented both numerically and qualitatively (i.e. from worst to best). The Table 1 represents an attributes and values that will be used in this questionnaire.

Table E.1. Attributes of the research and its values for 50 meters.

Attribute Measurement	Value variation	
	Worst	Best
X_1 – Potential power output *MWh/year*	$\diamond\diamond_1^0 = 0$	$\diamond\diamond_1^* = 59\,708$
X_2 – GHG reduction potential *tCO2eq/year*	$\diamond\diamond_2^0 = 1127$	$\diamond\diamond_2^* = 3239$

For instance, in case of attribute X_1 – Potential power output the x^* means the best value, max power output from a wind turbine under optimal conditions, and the x^0 the worst possible value of power output from a wind turbine.

Please answer the questions on the next pages, your valuable answers in decision-making process through this questionnaire will play an important role in advancing the understanding of the intricate relationship between these attributes, contributing to the optimization of WPP locations. The data obtained will be used only within the framework of this scientific research.

Question #1. Assess the dependence of X_1 – Potential power output from X_2 – GHG reduction potential

a) Given two projects A and B with a 50/50 chance of getting different energy generation from a wind turbine, which project would you prefer?

Scenario 1. In this scenario both projects have the fixed GHG reduction potential which is equal to $\diamond\diamond_2^0$ = **1127** *tCO2eq/year.*

Project A Project B

$\diamond\diamond_1^{*}$ = *59 708 MWh/year*	$\diamond\diamond_1^{''}$ = *50 751 MWh/year*
$\diamond\diamond_1^{0}$ = *0 MWh/year*	$\diamond\diamond_1^{'}$ = *8956 MWh/year*

Circle one out of three choices:

Project A *I'm indifferent (the projects are equivalent)* *Project B*

b) Which project would you prefer in the next scenario?

Scenario 2. If in both projects the value will be $\diamond\diamond_2^{*}$ = **3239** *tCO2eq/year.*

Project A Project B

$\diamond\diamond_1^{*}$ = *59 708 MWh/year*	$\diamond\diamond_1^{''}$ = *50 751 MWh/year*
$\diamond\diamond_1^{0}$ = *0 MWh/year*	$\diamond\diamond_1^{'}$ = *8956 MWh/year*

Circle one out of three choices:

Project A *I'm indifferent (the projects are equivalent)* *Project B*

c) If the value of attribute X_2 in scenario 1 or 2 were held fixed at some other value between 1127 and 3239 tCO2eq/year, would your answer change?

Circle your answer: *Yes No*